The Pennsylvania State University

The Graduate School

College of Earth and Mineral Sciences

THE EFFECT OF OZONOPAUSE PLACEMENT ON TROPOSPHERIC OZONE BUDGETS: AN ANALYSIS OF OZONESONDE PROFILES FROM SELECTED IONS-06 SITES

A Thesis in

Meteorology

by

Kerry Meaghan Dougherty

Submitted in Partial Fulfillment
of the Requirements
for the Degree of

Master of Science

May 2008

The thesis of Kerry Meaghan Dougherty was reviewed and approved* by the following:

Anne M. Thompson
Professor of Meteorology
Thesis Advisor

William F. Ryan
Faculty Research Assistant, Department of Meteorology

Hampton N. Shirer
Associate Professor of Meteorology

William H. Brune
Professor of Meteorology
Head of the Department of Meteorology

*Signatures are on file in the Graduate School

ABSTRACT

Identifying the tropopause is a significant challenge because it can be defined thermally, dynamically, or chemically. This study calculates ozonopauses using five methods that are each based on an ozone concentration cutoff, a best fit line, or an ozone gradient. The data set includes spring and summer ozonesonde launches from the IONS-06 campaigns in Narragansett, Rhode Island; Kelowna, British Columbia; and Houston, Texas. Variations in the ozonopause placements are dependent on season and site. On average, the five methods match most closely for the spring launches over Kelowna; the five methods differ the most for summer launches over Houston.

The five ozonopauses for each day yield five estimates of the total tropospheric ozone column (TTOC). Tropospheric ozone budgets are calculated by dividing each TTOC into four categories: boundary layer ozone, regional convection and lightning generated ozone, stratospherically injected ozone, and aged or recently advected ozone. The five budgets from each day are compared to assess the effect of ozonopause placement on tropospheric ozone budgets. Seasonal averages of the ozone budgets for each site indicate that the relative contributions of each term change by less than 5% of the TTOC. Daily comparisons can lead to higher differences on days for which there are large variations in ozonopause placements.

TABLE OF CONTENTS

LIST OF TABLES

LIST OF FIGURES

ACKNOWLEDGMENTS

The data used in this thesis were obtained in 2006 during the IONS (INTEX Ozonesonde Network Study) field campaigns supported by the NASA INTEX (Intercontinental Chemical Transport Experiment) project.

I would like to thank Anne Thompson for supporting me throughout the thesis process and Sonya Miller for sharing her programming expertise. I would also like to thank my committee members, Bill Ryan and Nels Shirer, for their input.

My current and former officemates from 423 Walker have been an amazing source of knowledge, support, and entertainment. Thank you, Jacquie, John, and Alaina!

Finally, I would like to extend a big thank you to the rest of my friends and family for sticking by me during this stressful process. I truly appreciate the phone calls, visits, care packages, and encouraging words. Thanks, y'all!

Chapter 1. INTRODUCTION

The INTEX (Intercontinental Chemical Transport Experiment) Ozonesonde Network Study (IONS) yielded over 700 profiles in the spring and summer of 2006. The ozonesondes, launched throughout North America during these campaigns, measured ozone concentrations throughout the troposphere and the lower stratosphere. An analysis of the tropospheric portion of the profiles is important because tropospheric ozone is a pollutant that has detrimental effects on human health (e.g. Bell *et al.* 2004).

The multitude of data requires an efficient and accurate method for determining the tropopause height with a computer algorithm. There is no strict definition for the tropopause, but this study investigates methods for calculating an ozonopause, a chemically defined tropopause. The total amount of ozone between the ground and the tropopause is the tropospheric ozone column (TTOC) that can be divided into boundary layer ozone and free tropospheric (FT) ozone. FT ozone is divided further using the laminar identification method developed by Stone and Thompson (Stone 2006; Thompson *et al.* 2007a,b). Tropospheric ozone budgets quantify the contributions of each ozone source as described in Section 1.1.

In this study, there are two main objectives: (1) to find an accurate algorithm to define the ozonopause and (2) to investigate the effect of the ozonopause placement on tropospheric ozone budgets. Multiple tropopause definitions are discussed in Section 1.2. Out of 23 IONS-06 sites, three are chosen for this study: Narragansett, Rhode Island;

Kelowna, British Columbia; and Houston, Texas. Section 1.3 discusses characteristics of these sites and why they are selected.

Chapter 2 describes the data and methods used in this thesis. Chapter 3 reveals and discusses the results from the ozonopause investigation, and Chapter 4 summarizes and suggests future directions for the research.

1.1 Lamina-labeling of Ozone Profiles

Lamina-labeling of ozone profiles is the first step in calculating tropospheric ozone budgets. Dobson (1973) describes a layering effect of ozone at high latitude sites in the spring. He refers to the maxima and minima in ozone concentrations as ozone laminae. Teitelbaum *et al*. (1996) confirms the presence of ozone laminae in Arctic sites. Reid and Vaughn (1991) indicate that ozone laminae are seen only in sites north of 30 ^{o}N and south of 30 ^{o}S, mainly in the winter and spring. Grant *et al.* (1998), Loucks (2007), and Thompson *et al.* (2007a, b) dispute this finding with evidence that ozone laminae are present in the tropics and subtropics and in the summer. Figure 1 demonstrates the laminar structure of ozone from a summertime ozonesonde launch over Houston.

The alternating increases and decreases in ozone mixing ratio are thought to be created through horizontal transport by Rossby waves and vertical transport by gravity waves (Pierce and Grant 1998). Teitelbaum *et al*. (1996) find that ozone laminae are correlated with potential temperature. Rossby wave transport occurs generally parallel to

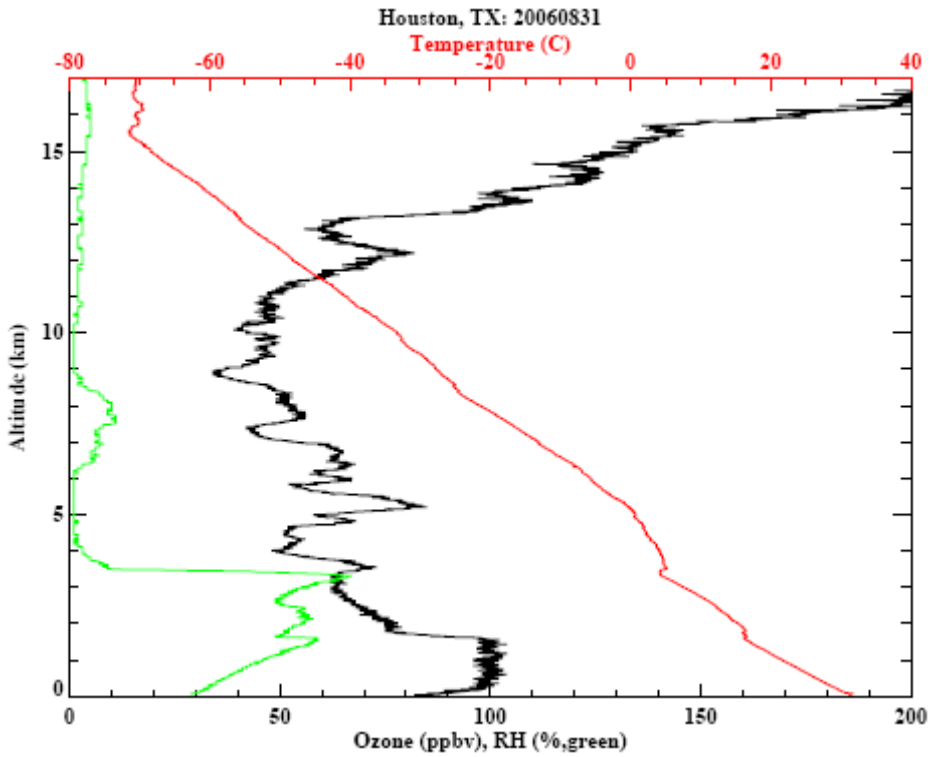

Figure 1. A sounding from August 31, 2006 over Houston, TX. Distinct layers are visible in the ozone mixing ratio (black).

constant potential temperature surfaces, and so ozone laminae created by Rossby waves are *not* correlated with potential temperature perturbations (Holton 1987). Gravity wave transport occurs generally perpendicular to constant potential temperature surfaces, and so ozone laminae created by gravity waves are correlated with potential temperature perturbations (Holton 1987).

Rossby wave laminae are associated with stratospheric injection of ozone into the troposphere, and gravity wave laminae are associated with convection that draws ozone and ozone precursors from the boundary layer (Teitelbaum 1996, Stone 2006). This

laminar identification (LID) method is used in multiple studies in northeastern North America (Pierce and Grant, 1998; Stone 2006; Thompson *et al.* 2007; Yorks 2007) and in the tropics (Loucks 2007).

This thesis applies LID to spring and summer data from three sites that range from 29.7 ^{o}N to 49.9 ^{o}N. The method is discussed further in Chapter 2. The next section describes the categorization of tropospheric ozone and sources of free tropospheric ozone.

1. 2 Categorization of Tropospheric Ozone

Thompson *et al.* (2007) apply the LID method created by Teitelbaum (1996) and Pierce and Grant (1998) to divide the tropospheric ozone column into four categories: (1) boundary layer (BL) ozone, (2) regional convection and lightning generated (RCL) ozone, (3) stratospherically injected (Strat) ozone, and (4) recently advected or aged (Adv) ozone. The four categories are depicted in Fig. 2.

The first category of ozone is boundary layer ozone. Ozone mixing ratios are higher in the boundary layer than in the free troposphere, primarily due to the anthropogenic emissions of NO_x ($NO + NO_2$) and hydrocarbons (VOCs) near the surface (Baird and Cann 2005). Reactions 1-3 occur together in the troposphere and comprise a null cycle that leads to no net production of ozone.

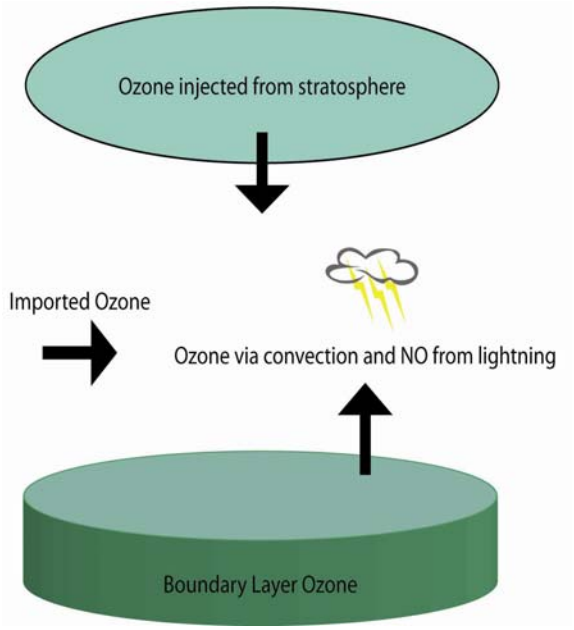

Figure 2. (Adapted from Stone 2006) A schematic summary of four categories of tropospheric ozone.

$$NO_2 \xrightarrow{UV} NO + O \qquad \text{Reaction 1}$$

$$O + O_2 \rightarrow O_3 \qquad \text{Reaction 2}$$

$$O_3 + NO \rightarrow NO_2 + O_2 \qquad \text{Reaction 3}$$

Reaction 2 is the only known way to produce ozone in both the troposphere and the stratosphere. Reaction 1 proceeds with a photon that has a wavelength less than 424 nm. Oxygen atoms in the troposphere do not originate from the photochemical decomposition of diatomic oxygen because stratospheric ozone filters out the high energy photons necessary to break the strong bond between the oxygen atoms (Baird and Cann 2005).

High concentrations of ozone in the boundary layer develop when Reaction 3 from the null cycle shown above is interrupted. Hydrocarbons in the boundary layer react with hydroxyl radicals to form catalytic radicals that replace ozone in Reaction 3. The result is that NO_2 is formed without the destruction of ozone, and Reactions 1 and 2 proceed to produce more ozone. Enhancements of boundary layer ozone are seen in highly industrialized areas and highly populated areas with heavy traffic, such as Houston (Morris *et al.* 2006).

The second category of tropospheric ozone is regional convection and lightning generated ozone that can be seen in the middle and upper troposphere. This ozone is attributed to gravity waves in the LID from Section 1.1. Regional convection lifts boundary layer ozone and ozone precursors into the free troposphere. Multiple studies demonstrate that lightning is the dominant source of NO_x in the middle and upper troposphere (Bond *et al.* 2001; Zhang *et al.* 2003; Choi *et al.* 2005). Kaynak *et al.* (2008) propose that lightning accounts for up to 30% of total NO_x emissions in the United States. Hudman *et al.* (2007) and Kaynak *et al.* (2008) identify high concentrations of lightning NO_x over the southeastern United States and Texas. NO_x forms ozone through the same reactions that occur in the boundary layer. Cooper *et al.* (2006) attribute 69-84% of the ozone enhancement over North America during the IONS-04 campaign period to lightning.

The third category of tropospheric ozone is stratospherically injected ozone. This ozone is attributed to Rossby waves in the LID from Section 1.1. Findings from Merrill *et al.* (1996) support the Rossby wave classification by Teitelbaum (1996) and point to the breaking of Rossby waves as a source of stratospherically injected ozone in the summer over Bermuda. Postel and Hitchman (1999) find similar results in the subtropics. Thompson *et al.* (2007b) indicate that ozone with stratospheric origins composes 20-25% of the TTOC over northeastern North America during the IONS-04 campaign period.

The fourth category of tropospheric ozone is recently advected or aged ozone. This category represents the residual of the TTOC when the other three categories are subtracted. It includes background ozone as well as ozone that is transported horizontally with weather systems. Recently advected or aged ozone is the final category required to calculate the daily tropospheric ozone budgets discussed in Chapter 3.

1.3 Tropopause Placement

Although the tropopause often is described as a transition *region* between the troposphere and the stratosphere (e.g. Birner 2006), tropospheric ozone budgets require an exact tropopause height. Ozone is integrated from the ground to the tropopause to determine the TTOC. Variations of 1-2 km in the placement of the tropopause can lead to differences of 10-20% in the TTOC (Stajner *et al.* 2008). If the TTOC is placed too high, then the TTOC will include some ozone in the stratosphere. A difficulty that arises with tropopause placement is the multitude of tropopause definitions. For example, Postel and

Hitchman (1999) designate a dynamically defined tropopause using the +/- 1.5 potential vorticity (PV) unit (10^{-6} K m^2 s^{-1} kg^{-1}) contour. The World Meteorological Organization (WMO 1957) designates a thermally defined tropopause as the bottom bound of a layer that has a lapse rate of less than 2 K km^{-1} for at least 2 km. Finally, Hsu and Prather (2005) designate a chemically defined tropopause as the height where the ozone concentration reaches 100 ppbv. Many studies document the differences in the tropopause heights that result from variations in the tropopause definitions (e. g. Hoerling *et al.* 1991).

Stajner *et al* (2008) uses assimilated ozone data from satellite measurements to investigate the differences in the TTOC that arise when the tropopause is defined dynamically, thermally, or chemically. The dynamic and thermal tropopauses are determined using similar methods as those described above. The chemical tropopause is determined in two ways: (1) starting at 500 hPa and increasing in height until the ozone concentration reaches 100 ppbv, and (2) starting at 51 hPa and decreasing in height until the ozone concentration reaches 100 ppbv. Figure 3 summarizes the results. The majority of the IONS-06 sites lie between 30 ^{o}N and 60 ^{o}N where the average tropopause heights, determined by the four tropopause definitions, are most divergent. The tropopause height differences lead to TTOC differences in the area between 30 ^{o}N and 60 ^{o}N.

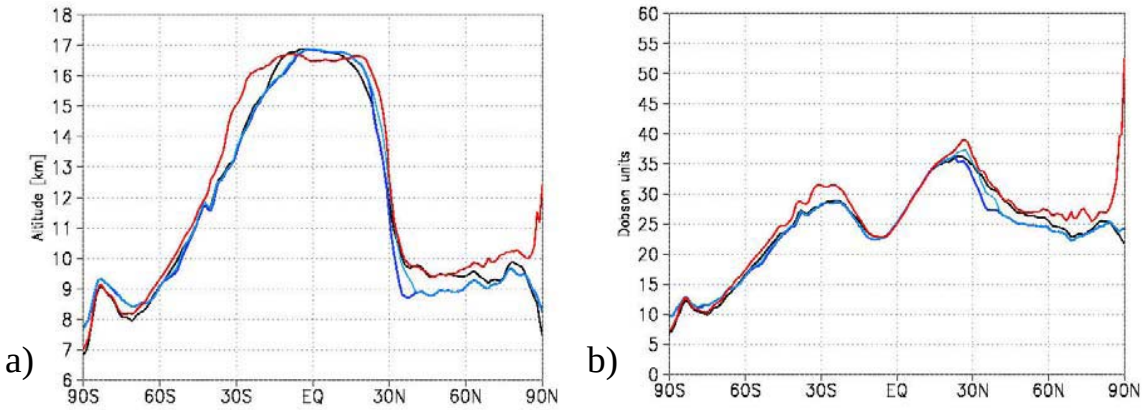

Figure 3. (From Stajner et al. 2008) a) Average tropopause height on February 15, 2005 given by four tropopause definitions: dynamic (black), thermal (red), ozone from below (blue), ozone from above (light blue). b) Corresponding average TTOC for the four tropopause definitions.

The tropopause investigation in this thesis is motivated by these results. The investigation focuses on multiple methods for calculating an ozonopause that separates high concentrations of stratospheric ozone from lower concentrations of tropospheric ozone. The two chemical tropopauses from Stajner *et al*. (2008) are used as well as three others that are described in Chapter 2. Three research questions addressed in Chapter 3 are:

1) Which of the five methods is the most accurate at placing the ozonopause?

2) Do the five methods lead to similar ozonopause heights?

3) If the ozonopause heights are different, then do the percentages of BL, RCL, Strat, and Adv ozone stay the same?

1.4 Introduction to Selected IONS-06 Launch Sites

The IONS-06 field campaigns launched ozonesondes at 23 sites (see Fig. 4) that ranged from 13.2 ^{o}N to 53.6 ^{o}N. Narragansett, Rhode Island (7); Kelowna, British Columbia (1); and Houston, Texas (19) are chosen for analysis in this thesis. The three sites lie in areas where the four tropopause definitions from Stajner *et al*. (2008) diverge. The sites represent a variety of climates, latitudes, and elevations. Spring and summer ozonesonde launches were conducted at the three sites to allow for a seasonal investigation.

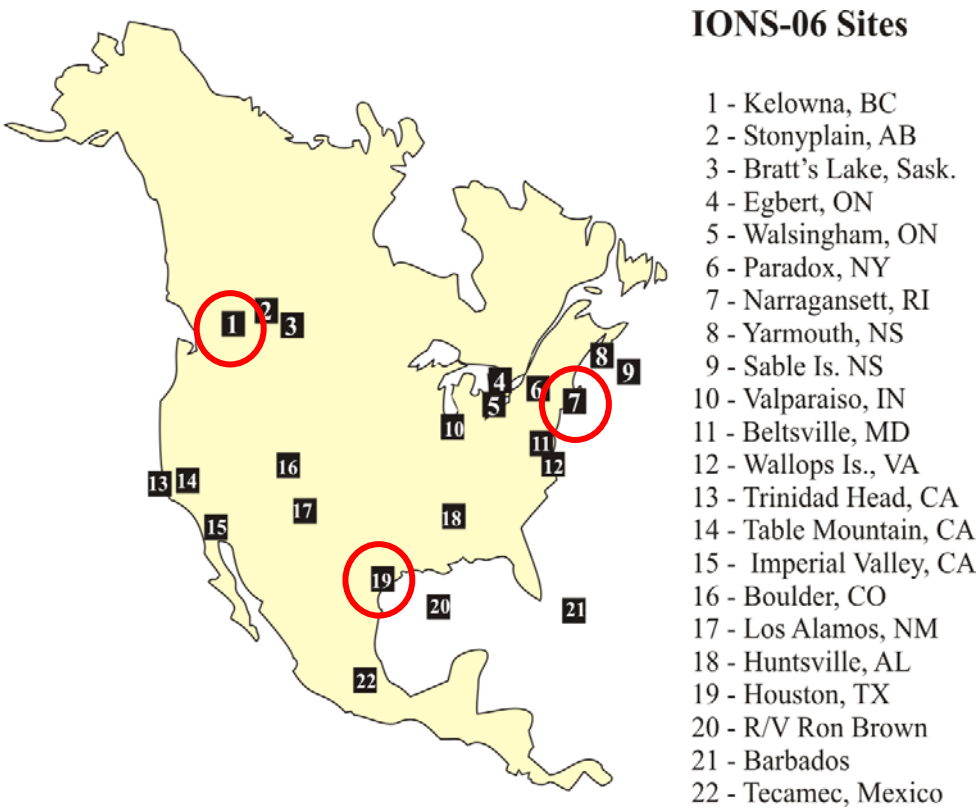

Figure 4. (From http://croc.gsfc.nasa.gov/intexb/ions06) A map of the 23 IONS-06 launch sites. The three sites used in this study are circled in red.

Narragansett, Rhode Island (41.5 ^{o}N, 71.4 ^{o}W) is a beach town with approximately 16,000 (U.S. Census 2000) residents. Owing to the small population, one can assume that car traffic is low as well as the total NO_x emissions from the car traffic. The town is, however, downwind from New York City and Washington, D.C., high-ozone areas due in part to population density and car traffic. The elevation of the launch site in Narragansett is 21 m, and the topography around the site is flat. During the spring (March/April/May), the average high temperature is 57 ^{o}F; the average low temperature is 36 ^{o}F. In August, the average high temperature is 80 ^{o}F; the average low temperature is 59 ^{o}F (The Weather Channel).

Kelowna, British Columbia (49.9 ^{o}N, 119.4 ^{o}W) is a fast-growing city with a current population of 107,000 (Statistics Canada 2006). The city is located in the Okanagan Valley, within the Columbian mountains (highest peaks around 3000 m). This location is significant because pollutants can become trapped in the valley and lead to high ozone levels. The elevation of the launch site in Kelowna is 456 m. Kelowna is the most continental of the three sites, and it has the highest latitude. During the spring, the average high temperature is 58 ^{o}F; the average low temperature is 33 ^{o}F. In August, the average high temperature is 81 ^{o}F; the average low temperature is 49 ^{o}F (The Weather Channel). Kelowna is the driest of the three sites, receiving less than 25% of the average yearly amount of precipitation seen in Narragansett and Houston. On average, there are only 0.90 in of precipitation in the spring and 1.30 in of precipitation in August.

Houston, Texas (29.7 ^{o}N, 95.4 ^{o}W) is the fourth-largest city in the United States with a current population of approximately 2.14 million (U. S. Census 2000). The elevation of the launch site is 19 m, and the topography around the site is flat. During the spring, the average high temperature is 80 ^{o}F; the average low temperature is 61 ^{o}F. In August, the average high temperature is 93 ^{o}F; the average low temperature is 75 ^{o}F (TWC). Emissions from car traffic and petrochemical industries contribute to high NO_x levels. The city lies in an area that is consistently in violation of the eight-hour standard for ground-level ozone (Texas Commission on Environmental Air Quality).

The next chapter describes the data and methods used for this thesis.

Chapter 2. DATA AND METHODOLOGY

The profiles used in this study were obtained with ECC (electrochemical concentration cell) ozonesondes and P-T-U (pressure-temperature-humidity) radiosondes launched with weather balloons. Although there were multiple launches on some days, only one launch per day is included in the analysis. The chosen launches took place in the afternoon, between 18 UTC and 23 UTC, depending on the time zone of the site. Table 1 summarizes the data set for the three sites.

Table 1. Date range and number of profiles by season for Narragansett, Kelowna, and Houston.

2006		Narragansett	Kelowna	Houston
Spring	Date range	Mar 8 - May 12	Mar 8 - May 17	Mar 1 - May 10
	# of profiles	n = 14	n = 28	n = 23
Summer	Date range	Aug 1 - Aug 30	Aug 2 - Aug 30	Aug 1 - Aug 31
	# of profiles	n = 28	n = 26	n = 16

Additional data used include: (1) backward air parcel trajectories (hereafter referred to as back trajectories) from the NOAA Air Resource Laboratory Hybrid Single-Particle Langrangian Integrated Trajectory (HYSPLIT) model (http://www.arl.noaa.gov/ready/open/traj.html) using the Eta Data Assimiliation System (EDAS) 40 km archived dataset and (2) Ertel's potential vorticity (EPV) calculated with the GEOS-4 model (Goddard Earth Observing Assimiliation Model, version 4).

The methodology is divided into three sections. The first two discuss the placement of the ozonopause and the planetary boundary layer; the third gives further details of the laminar identification method described in Chapter 1.

2.1 Determining the Ozonopause Height

Five ozonopause methods are compared to assess their effects on ozonopause height, the TTOC, and tropospheric ozone budgets. Three of the methods were developed for other studies, and two were developed for this thesis.

The first two methods for calculating the ozonopause are taken from Stajner *et al.* (2008) and are introduced in Section 1.3. In the first method, the search for the ozonopause begins at the altitude where the pressure equals 500 mb. The ozonopause is designated as the lowest altitude above the 500 mb level at which the ozone mixing ratio equals 100 ppbv. This method is labeled here as the cutoff-from-below method. In the second method, the search for the ozonopause begins at the altitude where the pressure equals 51 mb. The ozonopause is designated as the highest altitude below the 51mb level at which the ozone mixing ratio equals 100 ppbv. This method is labeled here as the cutoff-from-above method.

The third method for calculating the ozonopause is identical to the one used by Stone (2006) and Thompson *et al.* (2007a,b). With few exceptions, the ozonopauses for

all 23 IONS-06 sites lie between 7 and 20 km. A best fit line is created for the data points where the ozone is between 90 and 300 ppbv and the altitude is between 7 and 20 km. The height corresponding to 100 ppbv on the best fit line designates the ozonopause. This method is labeled here as the best-fit-line method.

In high altitude sites, such as Kelowna, the ozonopause is often close to 10 km, well below the 20 km cutoff used in the third ozonopause calculation from above. The best fit line is skewed by almost 10 km of data points that represent high concentrations of ozone in the stratosphere. The slope of the best fit line is too large and causes the ozonopause to be placed lower than it should be. Figure 5 depicts a case where this method fails. The calculated ozonopause is over 2 km below the actual ozonopause.

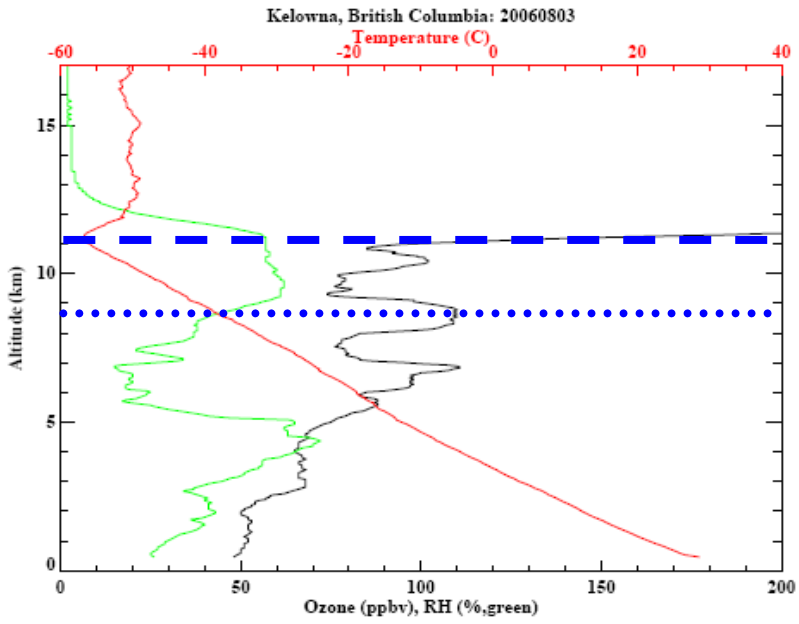

Figure 5. Sounding from Kelowna, British Columbia on August 3, 2006. The blue dotted line represents the ozonopause as calculated by the best-fit-line method; the blue dashed line represents a reasonable placement of the tropopause as determined by a visual assessment of the ozone mixing ratio (shown in black).

The best-fit-line method leaves room for improvement, and so a fourth method, using latitudinally based groups, is considered. Figure 6 demonstrates the correlation between latitude and ozonopause height when the ozonopause is calculated using the best-fit-line method. The average ozonopause height ranges from 16.4 km over Barbados (13.2 ^{o}N) to 9.6 km over Stonyplain (53.6 ^{o}N). Although some of the difference can be attributed to calculation error, generally an increase in latitude leads to a decrease in ozonopause height. Dividing the sites into latitudinally based groups allows for a smaller range of altitudes to be used in calculations for the best fit line, which should produce more accurate results. Figure 6 is used as a guideline for the grouping as well as visual assessments of ozonopause heights in curtain plots (see Fig. 7) of ozone mixing ratio.

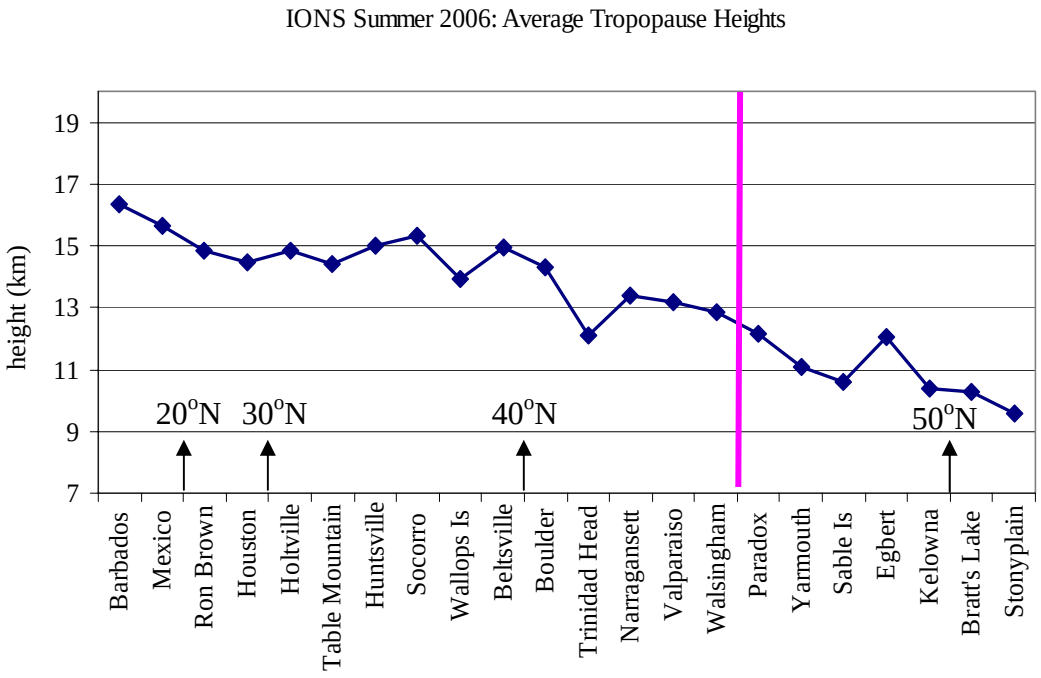

Figure 6. Average summer tropopause heights for 22 sites increasing in latitude from left to right. The pink line indicates the division between the northern and southern groups described above.

a)

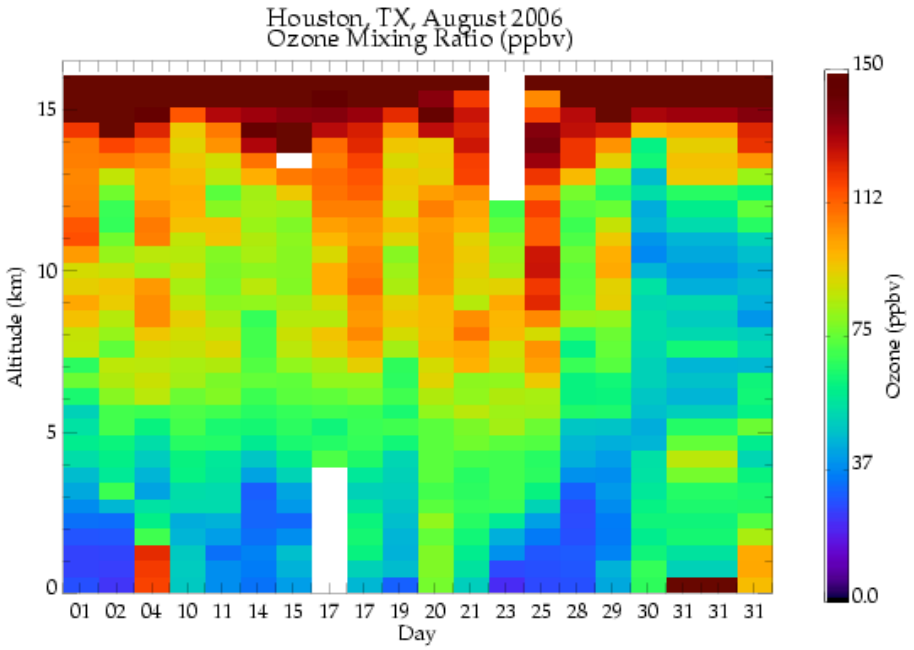

b)

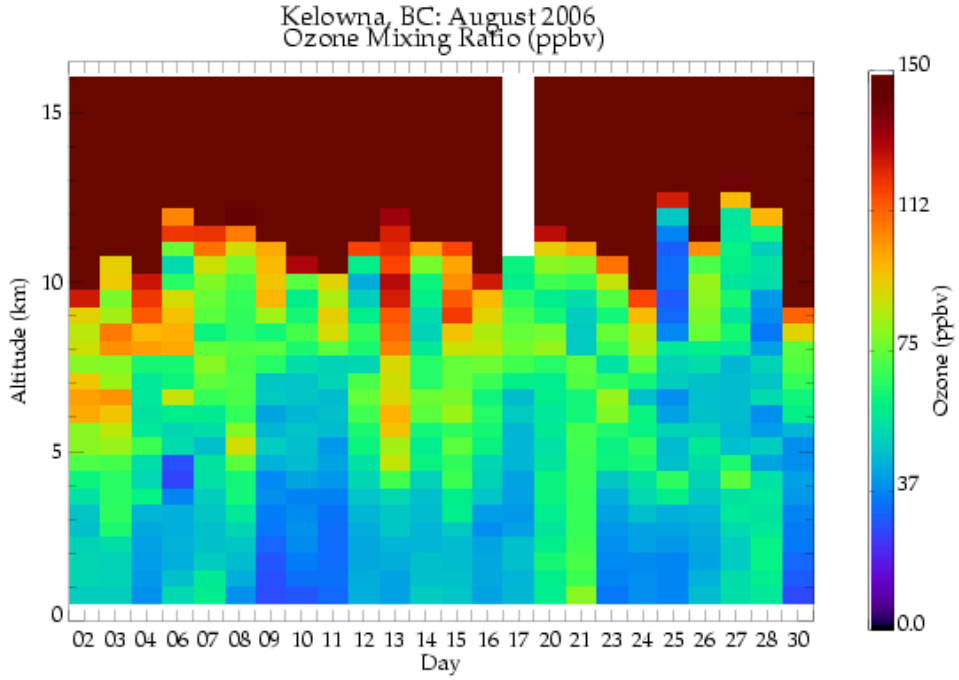

Figure 7. Curtain plots (obtained by averaging ozone concentrations every 0.5 km) visually demonstrate the latitudinal dependence of ozonopause height. The deep orange and red represent stratospheric ozone. **a)** Curtain plot of Houston (29.7 ^{o}N) ozone concentration concentrations in August 2006. **b)** Curtain plot of Kelowna (49.9 ^{o}N) ozone concentrations in August 2006.

Sites south of 43 ^{o}N are grouped together to form the southern group because they have curtain plots similar to the Houston plot in Fig. 7a. Sites north of 43 ^{o}N are grouped together to form the northern group because they have curtain plots similar to the Kelowna plot in Fig. 7b. The southern group has an average ozonopause of 15 km, and so the altitudes used for the cutoffs for the best fit line are 10 and 20 km. The northern group has an average ozonopause of 11 km, and so the altitudes used for the cutoffs are 7 and 15 km. Together the two groups span the entire 7 to 20 km range from the best-fit-line ozonopause method. In addition to the altitude changes, the ozone mixing ratio parameters are revised from the original calculation. The latitudinally based ozonopause calculation is performed in the same way as the best fit line ozonopause calculation. Considering only data points between the revised ozonopause altitudes, a best fit line is created for the data points where the ozone is between 100 and 200 ppbv. The height corresponding to 125 ppbv on the best fit line designates the ozonopause. This method is labeled here as the latitudinally-based-groups method.

The fifth and final method for calculating the ozonopause eliminates the use of a best fit line and relies on the sharp gradient in ozone mixing ratio near the ozonopause. Instead of the wide bounds used for the best fit line, the calculation uses a 0.5 km sliding window beginning at 5 km. The ozone concentration at 5 km is subtracted from the ozone concentration at 5.5 km. Then the window slides up 0.1 km and the same calculation is repeated for 5.1 km and 5.6 km. The calculations continue until the largest difference is found. After the appropriate window is located, the two altitudes are averaged to

determine the ozonopause height. If the ozone concentration ever drops below 100 ppbv above the determined ozonopause, then the calculation starts over from the ozonopause to identify the correct boundary between the troposphere and the stratosphere. This condition ensures that a large ozone spike in the lower troposphere is not identified as the ozonopause. Another condition added to the calculation is a 170 ppbv breaking point (i.e. the calculations stop if the ozone mixing ratio at the bottom edge of the window reaches 170 ppbv). This condition is necessary for cases where the ozone concentration does not completely level off. Figure 8 depicts one of these cases. In such cases, ozonopause placement is difficult regardless of the method used. This method is labeled here as the ozone-gradient method. Table 2 summarizes the five ozonopause calculation methods.

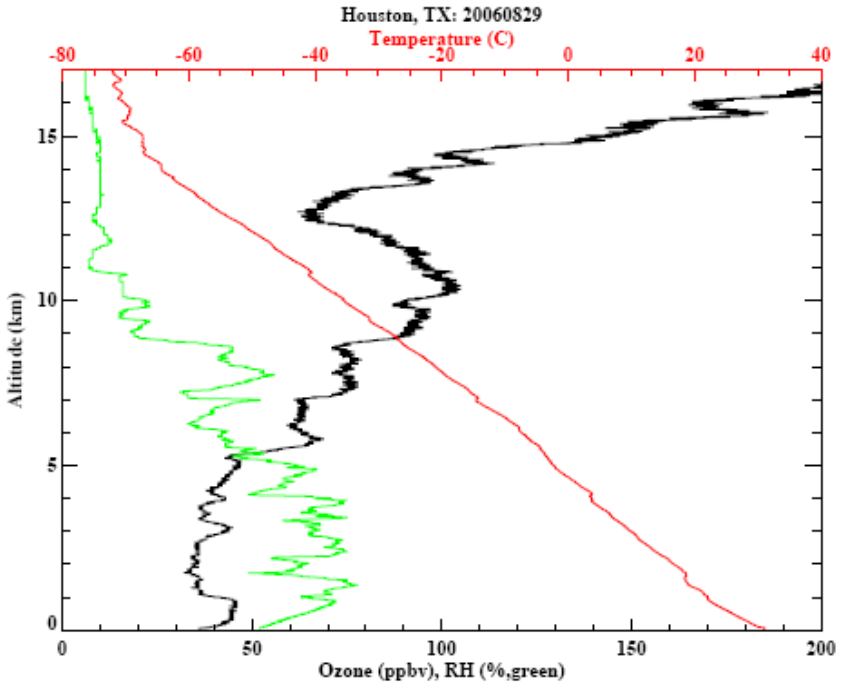

Figure 8. Sounding from Houston, TX on August 29, 2006 that does not show a distinct ozonopause.

Table 2. A summary of the five ozonopause methods described in Section 2.1.

Name of ozonopause method	Criterion	Search range
Cutoff-from-below	[ozone] = 100 ppbv	pressure < 500 mb
Cutoff-from-above	[ozone] = 100 ppbv	pressure > 51 mb
Best-fit-line	best fit line for [ozone] between 90 and 300 ppbv, cut best fit line at 100 ppbv	7- 20 km
Latitudinally-based-groups	best fit line for [ozone] between 100 and 200 ppbv, cut best fit line at 125 ppbv	7-15 km (north of 43 N) or 10-20 km (south of 43 N)
Ozone-gradient	0.5 km sliding window, average altitudes with largest difference in [ozone]	height > 5 km

2.2 Determining the Planetary Boundary Layer Height

The planetary boundary layer (PBL) height separates the boundary layer from the free troposphere in the LID method. For this thesis, initially three methods are attempted to place the PBL. The first PBL method used in LID is to assume the top of the PBL is 1 km above ground level (AGL) at all sites on all days. This method is identical to the method used by Stone (2006) and Thompson *et al.* (2007 a,b). The 1 km depth is selected based on a boundary layer study in the Gulf of Maine (Angevine *et al*. 2006). The primary focus of the above publications is northeastern North America. Because this region is only a subset of the IONS-06 launch sites, more methods need to be considered.

The second method for calculating the top of the PBL is to find the most negative second derivative of equivalent potential temperature (Stull 1988; Yorks 2007).

Examples of this method are shown in Fig. 9. The decrease in equivalent potential temperature (theta-e) with height represents an unstable layer up to approximately 1 km in Fig. 9a. Then theta-e remains constant up to 3.5 km, indicating a well-mixed layer and the top of the planetary boundary layer. The PBL is deeper in Kelowna than in the northeastern North American sites from Stone (2006) and Thompson *et al.* (2007a,b) because of the complex terrain due to the mountains, hills, and valleys around Kelowna. Figure 9b is more representative of the theta-e profiles from Kelowna. Most theta-e profiles do not show signatures of a well-mixed layer.

a)

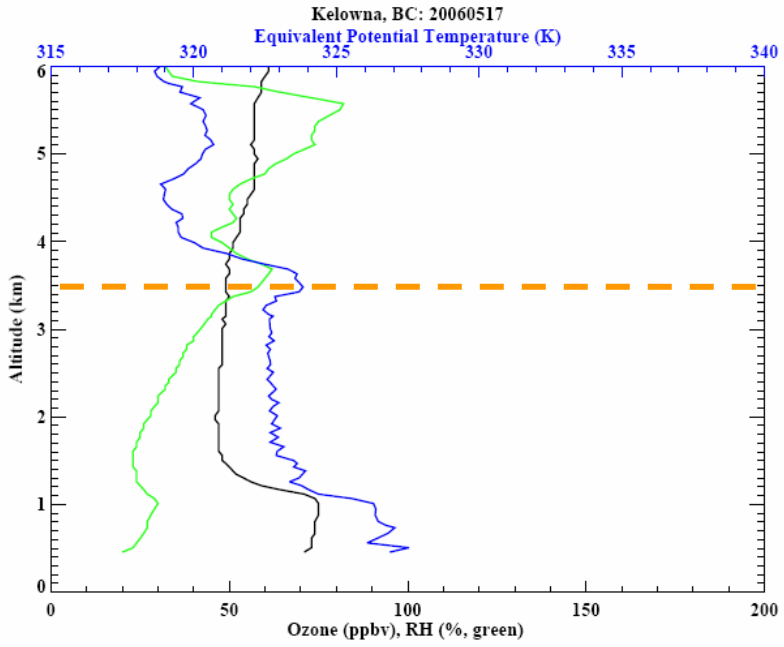

Figure 9 (a). Sounding from Kelowna with plot of equivalent potential temperature (shown in blue). The PBL height (orange) is clearly visible at the peak in theta-e.

b)

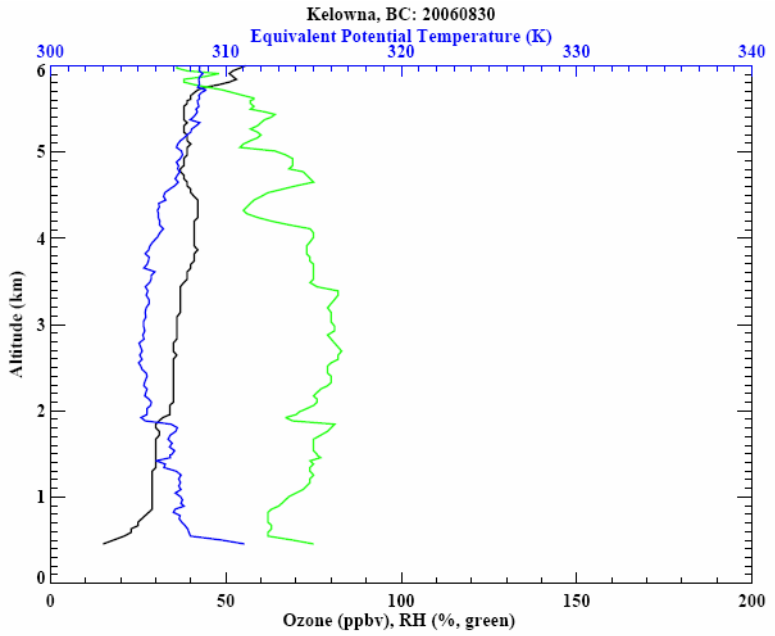

Figure 9 (b). Sounding from Kelowna with plot of equivalent potential temperature (shown in blue). The PBL height is not visible in the theta-e profile.

The third and final method identifies the top of the PBL using the peak in relative humidity (RH) near the surface. An example of this method is shown in Fig. 10. The top of the PBL in Fig. 10 is visible in the RH profile and the temperature profile. Ambiguous cases occur when there are multiple peaks in RH and no inversions in the temperature profile.

Each of the previously described methods leads to significant differences in the placement of the top of the PBL at Narragansett, Kelowna, and Houston. Figure 11 is included as an example of the variability given by these methods. Because of the shortcomings of each of the methods, this thesis uses seasonal estimates of the PBL instead of calculations.

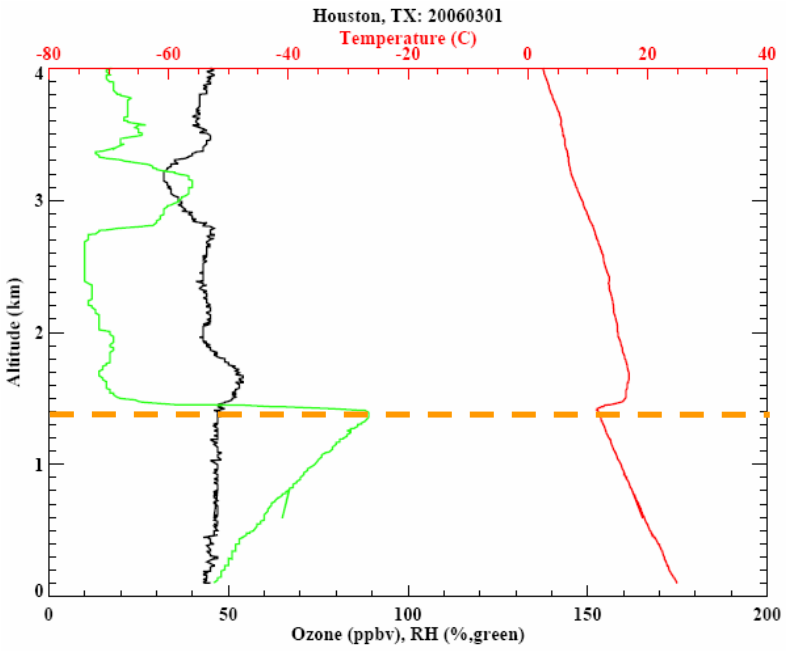

Figure 10. Sounding from Houston, TX on March 1, 2006. The top of the PBL (orange) is clearly visible in the RH profile and the temperature profile.

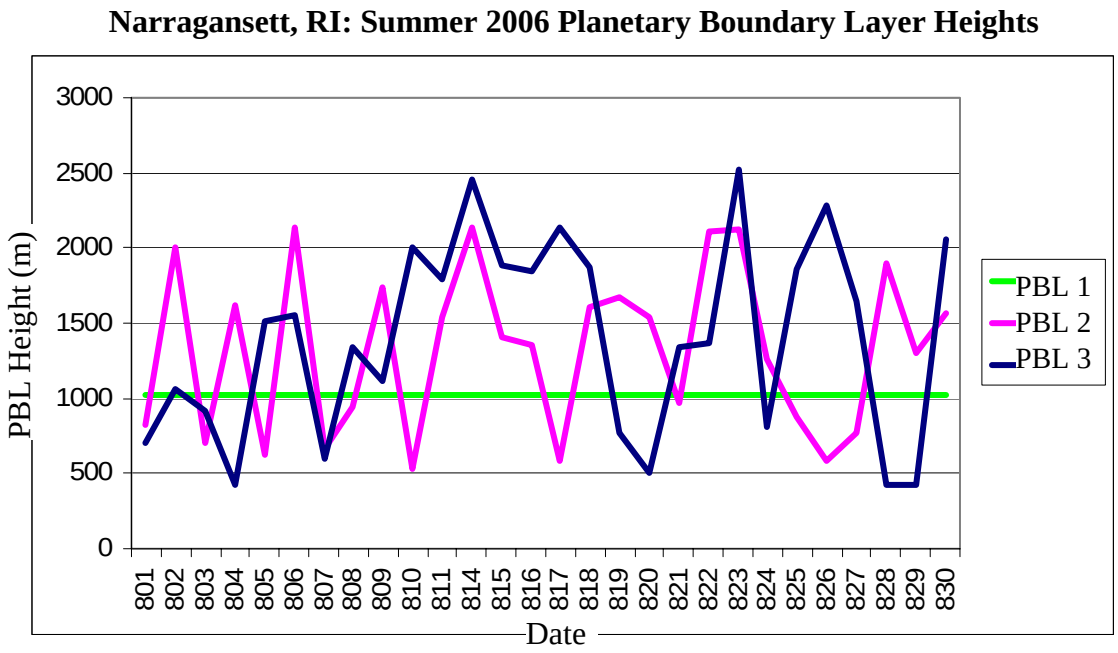

Figure 11. Summertime PBL heights (in meters) over Narragansett, RI, as determined by three methods. BL 1 (green) is the 1km method. BL 2 (pink) is the theta-e method. BL 3 (blue) is the RH method. See text for more details.

Seasonal estimates for the PBL heights over Narragansett and Houston are determined using mean profiles for each season. For these two sites, an average PBL height is seen in the RH and temperature profiles for spring and summer. Figure 12 is an example of the mean profiles.

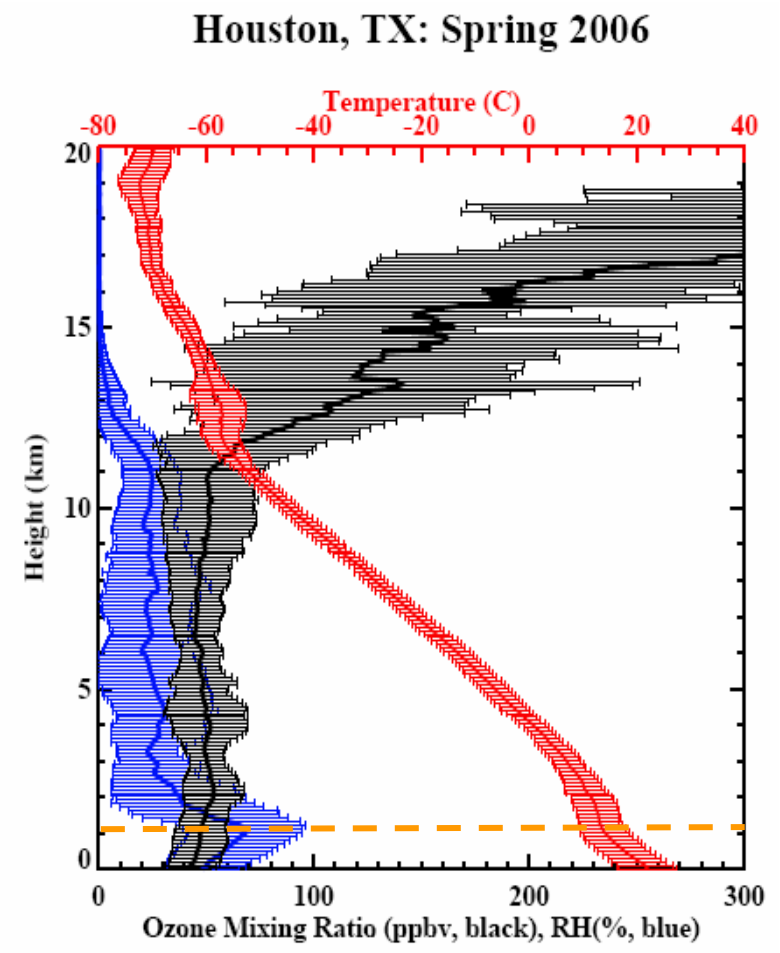

Figure 12. The mean profile for 23 launches over Houston in spring 2006. (The error bars represent one standard deviation.) The top of the PBL is estimated at 1km, based on the mean RH and mean temperature profiles.

The mean profiles for Kelowna do not show clear signatures of the PBL (e.g. Fig. 13). Holzworth (1972) calculated the PBL heights at 62 stations throughout the United States by identifying layers for which the lapse rate was approximately dry adiabatic. The PBL over Kelowna is estimated with the Holzworth PBL from Glasgow, Montana (48.1 ^{o}N, 106.4 ^{o}W), which is geographically and meteorologically similar to Kelowna, BC. Both sites are located in valleys within mountains of approximately the same height, and they are less than 2^{o} latitude apart. The elevation of Glasgow is approximately 100 m higher than the elevation of Kelowna. They are both dry sites with a similar range of temperatures in the spring and in the summer.

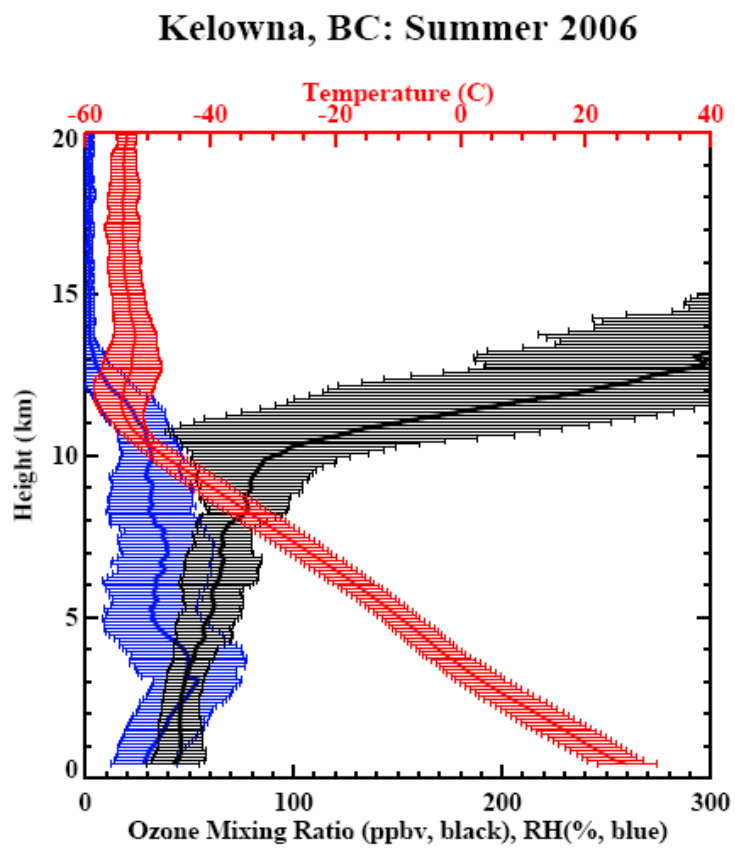

Figure 13. The mean profile for 26 launches over Kelowna in August 2006. The top of the PBL is difficult to determine using the mean RH and mean temperature profiles.

Based on the mean profiles and Holzworth (1972), the PBL heights used in the LID method in Chapters 3 are:

- Narragansett: spring – 1 km, summer – 1.5 km
- Kelowna: spring – 2.3 km, summer – 2.9 km
- Houston: spring – 1 km, summer – 1.5 km

2.3 Tropospheric Ozone Budgets

Tropospheric ozone budgets are calculated using LID, described in Section 1.1. The LID method uses correlations between ozone and potential temperature to identify layers as Rossby wave-induced (RW) or gravity wave-induced (GW), following the method used in Pierce and Grant (1998). In order to identify RW and GW layers, the original ozonesonde profiles are first linearly interpolated to create high resolution profiles. Each high resolution profile then is heavily smoothed by averaging the ozone concentrations over 2.5 km intervals. The result is a mean ozone profile. Next, the difference between the mean ozone profile and the high resolution profile is found, and this difference is divided by the mean profile to yield the normalized perturbation ozone mixing ratio. A normalized perturbation potential temperature is found using almost the same procedure as above. The only difference is the scale factor R(z), which is multiplied by the normalized perturbation potential temperature to yield a scaled perturbation potential temperature.

$$R(z) = \left(\frac{1}{O_3}\frac{\partial O_3}{\partial z}\right)\cdot\left(\frac{1}{\theta}\frac{\partial \theta}{\partial z}\right)^{-1} \qquad \text{(Pierce and Grant 1998)}$$

where O_3 is the mean ozone concentration, and θ is the mean potential temperature at some altitude z.

Next, the normalized perturbations of ozone mixing ratio are plotted with the scaled perturbations of potential temperature. The correlations between these two profiles are determined every 0.1 km for 5 km intervals. As discussed in Section 1.1, low correlations represent RW influence, and high correlations represent GW influence. Pierce and Grant (1998) quantify low correlations as -0.3 to 0.3; they quantify high correlations as greater than 0.7. The same cutoffs are applied in this thesis. Figure 14 is an example of the plots used in the LID method.

Tropospheric ozone budgets are calculated using the RW and GW classifications developed above. The TTOC is divided into four categories: (1) boundary layer (BL) ozone, (2) regional convection and lightning generated (RCL) ozone, (3) stratospherically injected (Strat) ozone, and (4) recently advected or aged (Adv) ozone. The TTOC is integrated up to the PBL heights determined in Section 2.2 to give the total amount of ozone in the BL. The remaining three categories compose the free troposphere. RCL ozone is associated with GW layers, and Strat ozone is associated with RW layers (see Section 1.2). Thompson *et al*. (2007a) reports a high correlation between gravity wave layers and RCL ozone. However, not all Rossby wave layers are indicative of stratospheric injection. For each layer identified as RW-induced by LID, relative

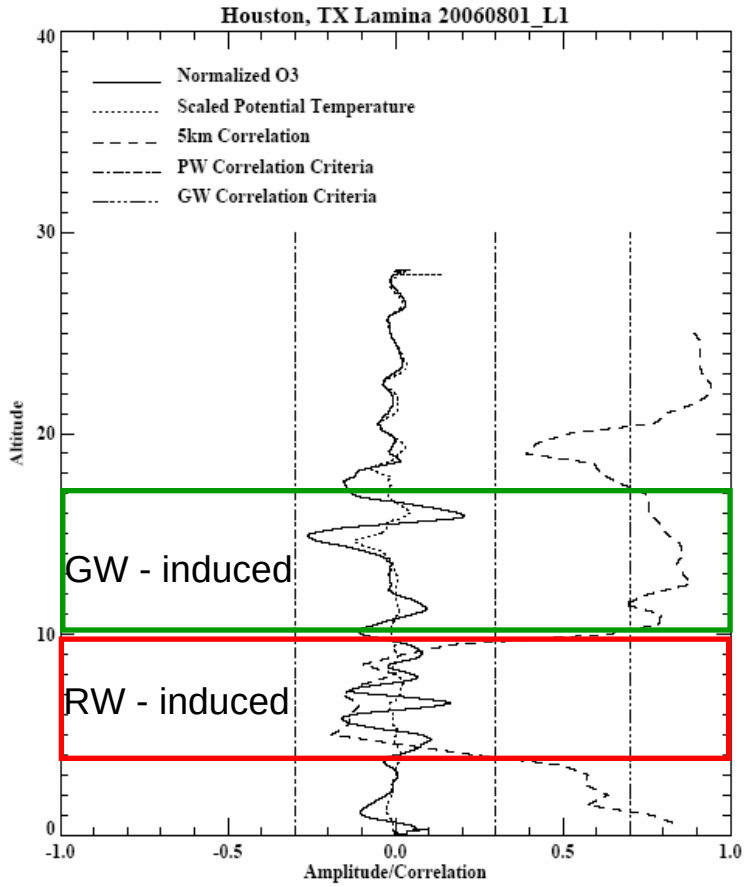

Figure 14. A sample perturbation sounding from Houston, TX on August 1, 2006. Ozone laminae in the red outlined box between 4 and 10 km show low correlations (dashed) between normalized ozone mixing ratio (solid) and scaled potential temperature (dotted). Ozone laminae in the green outlined box between 10 and 17 km show high correlations between normalized ozone mixing ratio and scaled potential temperature.

humidity, Ertel's potential vorticity (EPV), and back trajectories are analyzed for signs of stratospheric ozone. Low RH and back trajectories that pass through areas of high EPV indicate stratospheric origins. BL, RCL, and Strat ozone amounts are subtracted from the TTOC to yield the Adv ozone. These four terms constitute tropospheric ozone budgets. They are individually calculated for each profile, and they are averaged to show seasonal trends.

The TTOC used in the tropospheric ozone budgets is calculated using the five ozonopause methods that are described in Section 2.1. The ozone budgets that result from each method are compared in Chapter 3.

Chapter 3. RESULTS AND DISCUSSION

3.1 Comparisons of Ozonopause Heights

Figure 15 displays the ozonopause for each of the spring launches at Narragansett, Kelowna, and Houston. For each site, there are days with close agreement among all five methods, but there are also days for which the methods do not agree. The ozone-gradient (OG) method leads to the highest ozonopause in 82% of the spring ozonesonde launches. There are only four days at each site for which the OG method does not lead to the highest ozonopause. The cutoff-from-below (CFB) method leads to exceptionally low ozonopauses on May 10 in Narragansett and on three other spring days in Kelowna. The latitudinally-based-groups (LBG) method fails to provide an ozonopause estimate in Narragansett on March 22 and April 5. This method searches for ozone concentrations between 100 and 200 ppbv between 7 and 15 km, but on March 22 and April 5, the concentrations are well above 200 ppbv at 7 km. The profiles from these two days exhibit unusually low ozonopauses (below 7 km), which are likely a result of the cold fronts that passed through the eastern United States just before these two dates. Individual days with extreme outliers are analyzed later in this chapter.

Correlations between each method for each site are presented in Table 3. In Narragansett, the only pair of methods that are poorly correlated ($r < 0.5$) are the LBG and BFL (best-fit-line) method. This poor correlation is not surprising because the LBG method is a second version of the BFL method. It can be expected that when a method is

changed, the new method will give different results from the original. In Kelowna, all of the pairs of methods are well correlated. In Houston, the CFB and CFA (cutoff-from-above) methods are poorly correlated, indicating that the 100 ppbv cutoff to distinguish stratospheric ozone from tropospheric ozone is not sufficient. Also, the OG method is poorly correlated with the CFB and BFL methods. The mean correlation for each table is calculated by averaging all of the correlations between non-identical methods. The mean correlations are 0.74 for Narragansett, 0.92 for Kelowna, and 0.62 for Houston. These relatively high correlations imply that the methods generally follow the same trends (i.e. the methods identify when the ozonopause is higher or lower than on the day before).

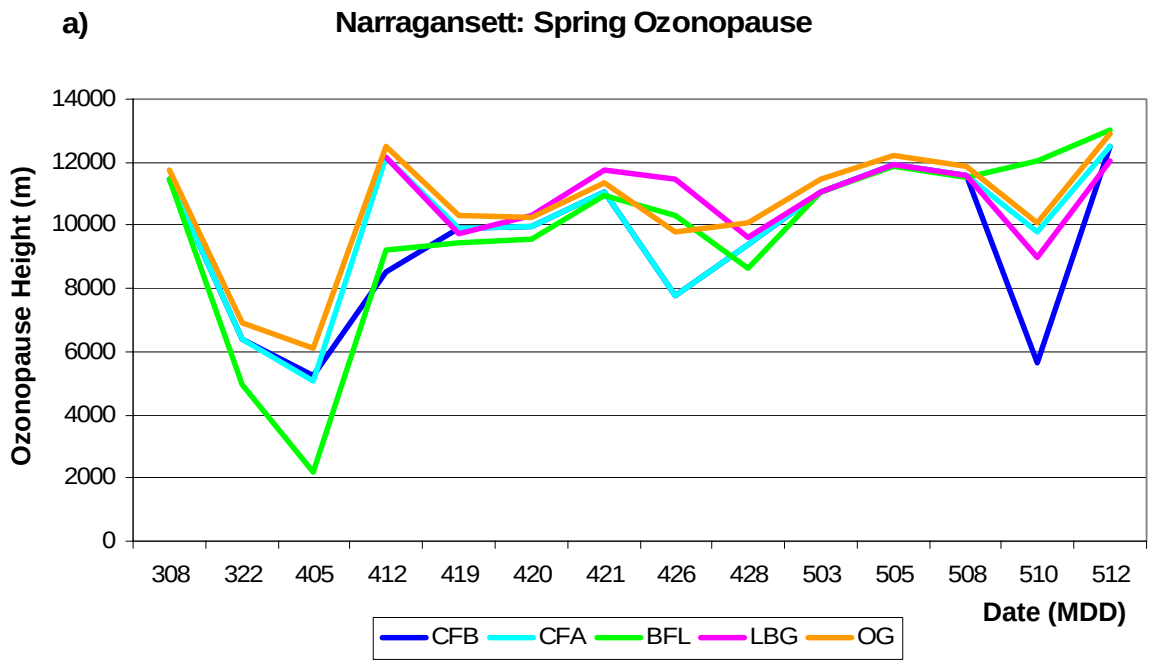

Figure 15 (a). Spring ozonopause heights determined by five different methods for Narragansett. CFB = cutoff-from-below method (dark blue), CFA = cutoff-from-above method (cyan) , BFL = best-fit-line method (green), LBG = latitudinally-based-groups method (pink), OG = ozone-gradient method (orange).

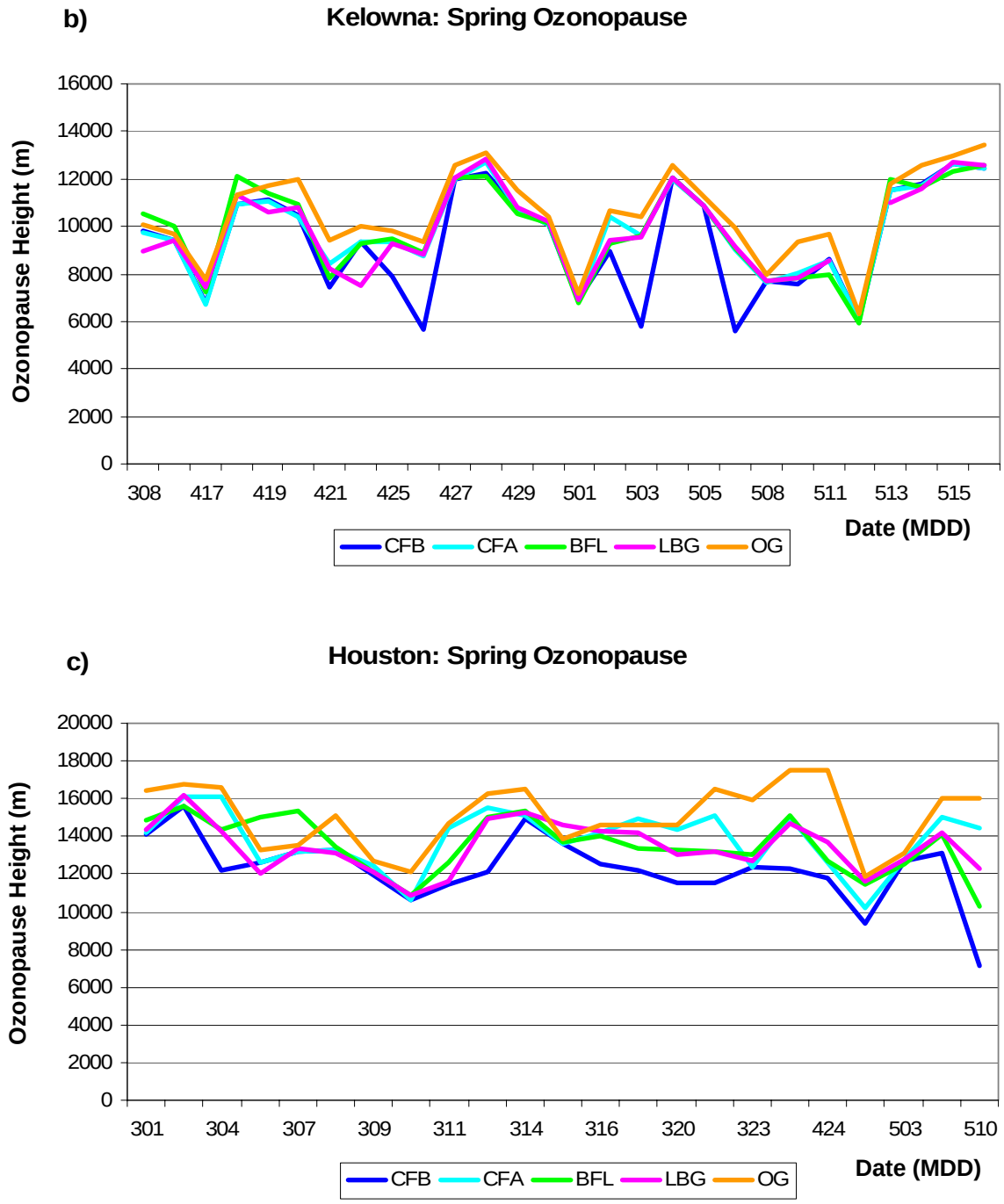

Figure 15 (b, c). Spring ozonopause heights determined by five different methods for Kelowna and Houston. CFB = cutoff-from-below method (dark blue), CFA = cutoff-from-above method (cyan) , BFL = best-fit-line method (green), LBG = latitudinally-based-groups method (pink), OG = ozone-gradient method (orange).

a) Narragansett spring: correlations between ozonopause methods

	CFB	*CFA*	*BFL*	*LBG*	*OG*
CFB	1.0				
CFA	0.8	1.0			
BFL	0.7	0.9	1.0		
LBG	0.6	0.6	**0.3**	1.0	
OG	0.8	1.0	0.9	0.8	1.0

b) Kelowna spring: correlations between ozonopause methods

	CFB	*CFA*	*BFL*	*LBG*	*OG*
CFB	1.0				
CFA	0.9	1.0			
BFL	0.9	1.0	1.0		
LBG	0.8	1.0	0.9	1.0	
OG	0.8	1.0	0.9	1.0	1.0

c) Houston spring: correlations between ozonopause methods

	CFB	*CFA*	*BFL*	*LBG*	*OG*
CFB	1.0				
CFA	**0.4**	1.0			
BFL	0.8	0.6	1.0		
LBG	0.7	0.8	0.8	1.0	
OG	**0.3**	0.7	**0.4**	0.7	1.0

Table 3. Correlations between ozonopause heights calculated from each of the five ozonopause methods for spring launches over Narragansett, Kelowna, and Houston. Bold values represent poor correlations ($r < 0.5$).

Correlations only reveal the similarities in trends between each of the five calculated ozonopauses for the three sites, and so standard deviations are needed to reveal the actual differences in ozonopause placement. For each ozonesonde launch, the five calculated ozonopauses are averaged together to determine a daily mean ozonopause. Then the daily standard deviation from the mean for each of the five ozonopauses is calculated. The standard deviations are divided into bins according to their frequency to create the histograms in Fig. 16. The histograms are useful for determining which site yields the least amount of variation between the five ozonopauses as well as determining outlier cases. The average standard deviation for Narragansett is 1.31 km (approximately 12% of the average ozonopause height), and the average standard deviation for Kelowna is 0.82 km (approximately 8% of the average ozonopause height). For Houston, the average standard deviation is 1.26 km (approximately 9% of the average ozonopause height). Based on these results, the five calculated ozonopauses are the most similar over Kelowna. An analysis of individual profiles is necessary to understand why the ozonopause methods lead to variations in ozonopause placements.

A day with large variations in ozonopause placements is May 10 in Narragansett. All of the methods except the BFL method indicate a decrease in ozonopause height from the previous launch (see Fig. 15a). Figure 17 is the sounding from this day. The ozonopause heights range from 5.7 km to 12.1 km with an average ozonopause of 9.3 km. There is a large spike in ozone concentrations around 6 km that provides the reason for the significant differences in ozonopauses heights. The CFB method picks up

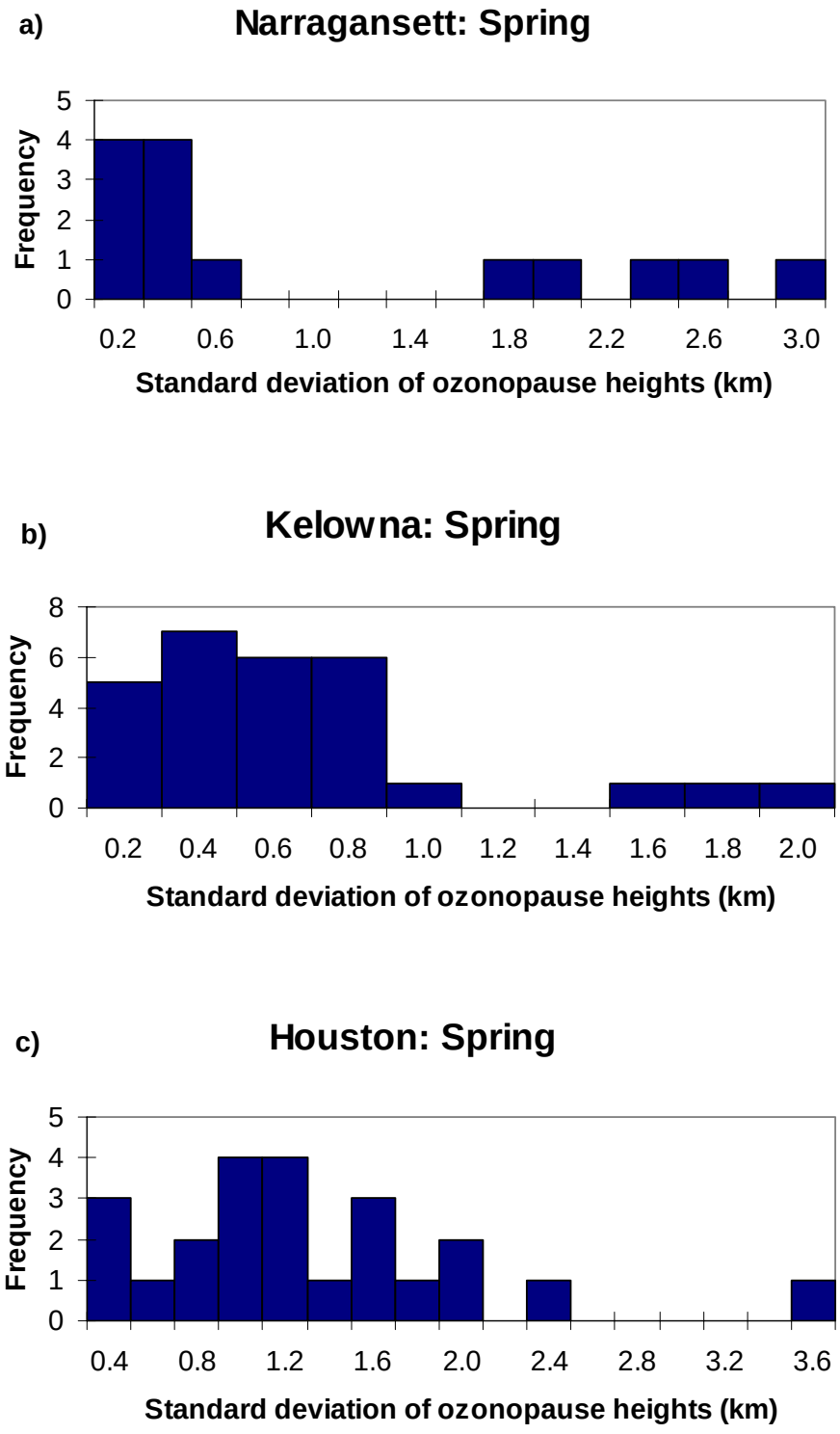

Figure 16. Histograms for Narragansett, Kelowna, and Houston that show the distributions of the standard deviations from the mean of the five ozonopauses in the spring.

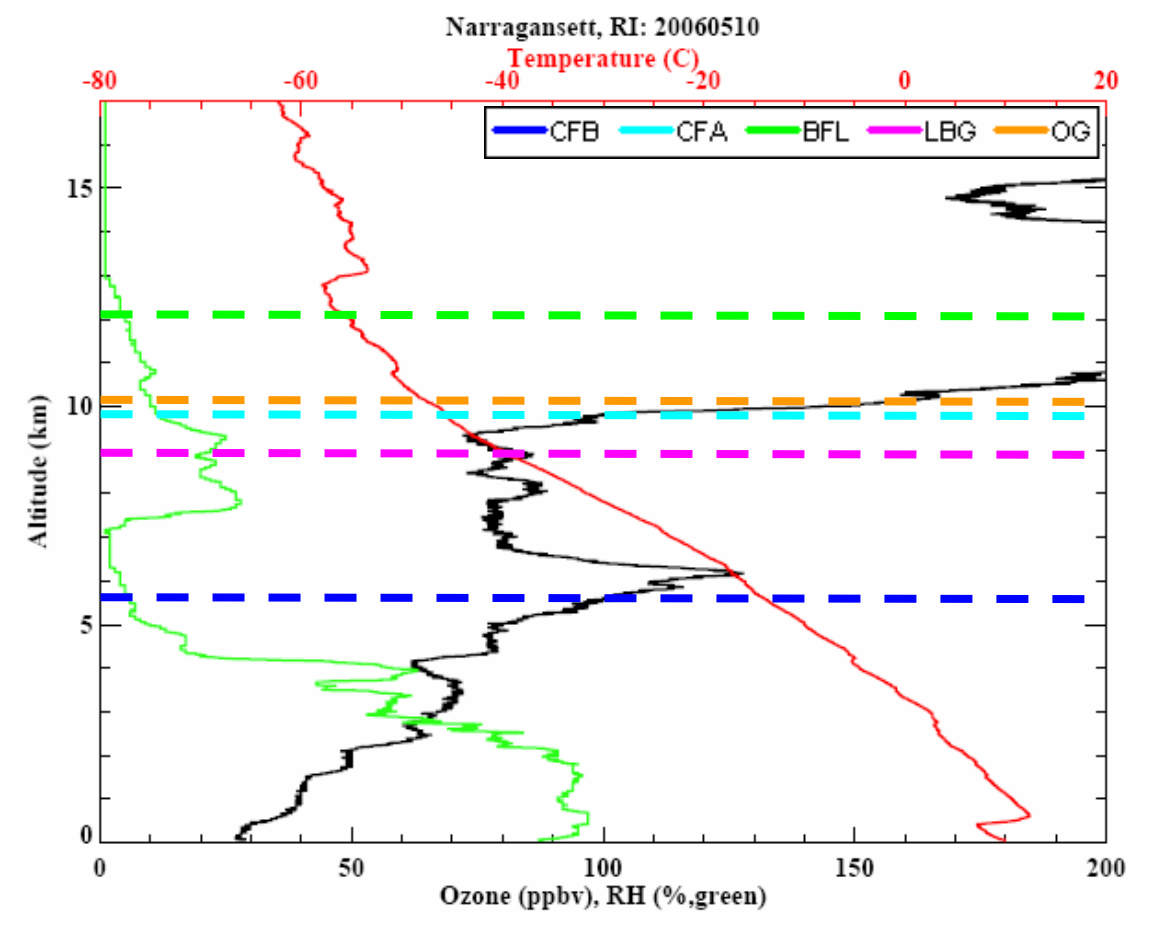

Figure 17. Sounding from Narragansett, RI on May 10, 2006. The ozonopauses calculated by five different methods are marked with dashed lines as denoted in the legend.

this ozone lamina as the ozonopause because the ozone concentrations within the layer exceed 100 ppbv. The LBG method improves the ozonopause placement by the BFL method, but both fail to identify the ozonopause. The OG method and the CFA method both place the ozonopause around 10 km, which is visually accurate based on the sharp gradient in the ozone concentrations.

Another interesting day is identified in Fig. 15b. On April 26 at Kelowna, all of the ozonopauses closely agree except for the CFB ozonopause. The ozone profile (Fig. 18) closely resembles the ozone profile in Fig. 17. They both have relatively low surface ozone, a peak in ozone around 6 km, and then a sharp gradient in ozone concentrations around 10 km. The peak in ozone around 6 km again causes the CFB method to place the ozonopause too low.

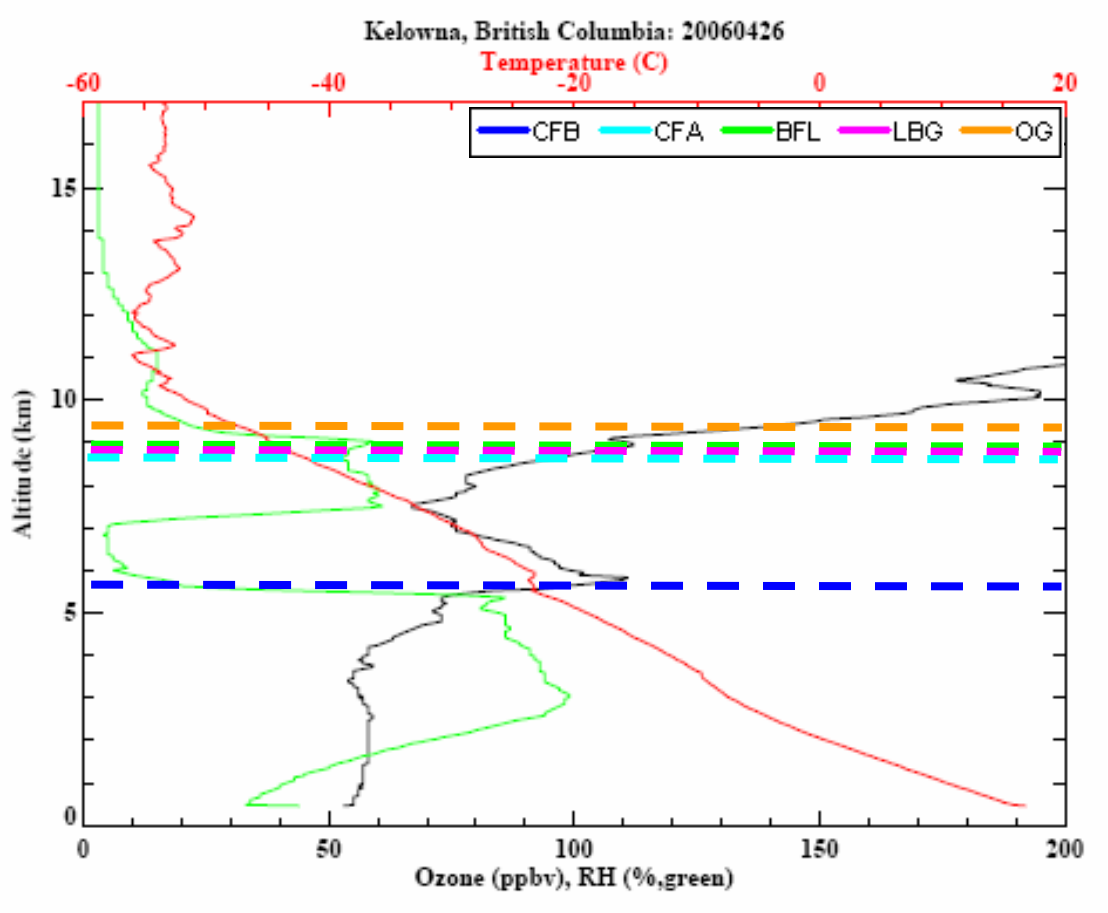

Figure 18. Sounding from Kelowna, BC on April 26, 2006. The ozonopauses calculated by five different methods are marked with dashed lines as denoted in the legend.

The largest differences in ozonopause heights occur at Houston. The two cases above demonstrate that large spikes in ozone concentrations create difficulties for some of the ozonopause calculation methods. The high concentrations of ozone can skew the best fit lines in the BFL and LBG methods, and they can cause the CFB method to place the ozonopause too low. Houston is known to have high levels of ozone owing to NO_x emissions from cars and the petrochemical industries, and so the variations in ozonopause placements are expected. Figure 19 depicts a day when the standard deviation from the mean of the five ozonopause heights is small (<1 km). There is a sharp gradient in the ozone concentrations that identifies the lower bound of stratosphere, and there are no altitudes in the lower troposphere that have ozone concentrations above 100 ppbv. Four of the ozonopause methods closely agree on the ozonopause placement. The only method that fails to pick up the unambiguous ozonopause is the BFL method, but this method is improved upon with the LBG method that accurately places the ozonopause.

The highest standard deviation of the spring launches comes from the launch over Houston on May 10. The average ozonopause height is 12.1 km and the standard deviation from the mean of the five methods is 3.5 km (29% of the average ozonopause). The LID method identifies the four ozone maxima seen in Fig. 20 as RW-induced. Analysis of the relative humidity profile in Fig. 20 points to stratospheric origins for the ozone laminae because the profile is dry above 7 km. The back trajectories in Fig. 21 indicate transport through high EPV areas (Fig. 22), also indicative of stratospheric-injection of ozone into the troposphere. In addition to the RH and EPV arguments for

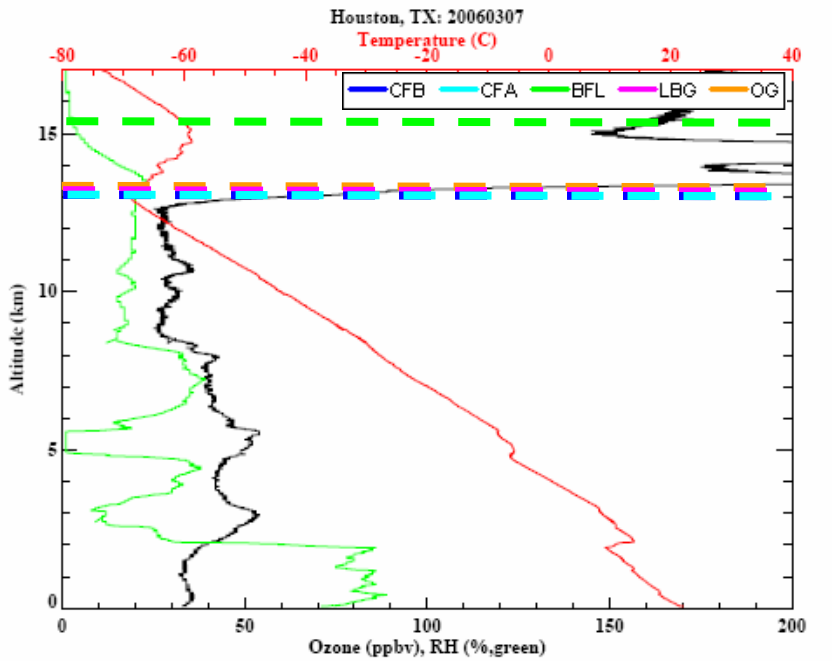

Figure 19. Sounding from Houston, TX on March 7, 2006. The ozonopauses calculated by five different methods are marked with dashed lines as denoted in the legend.

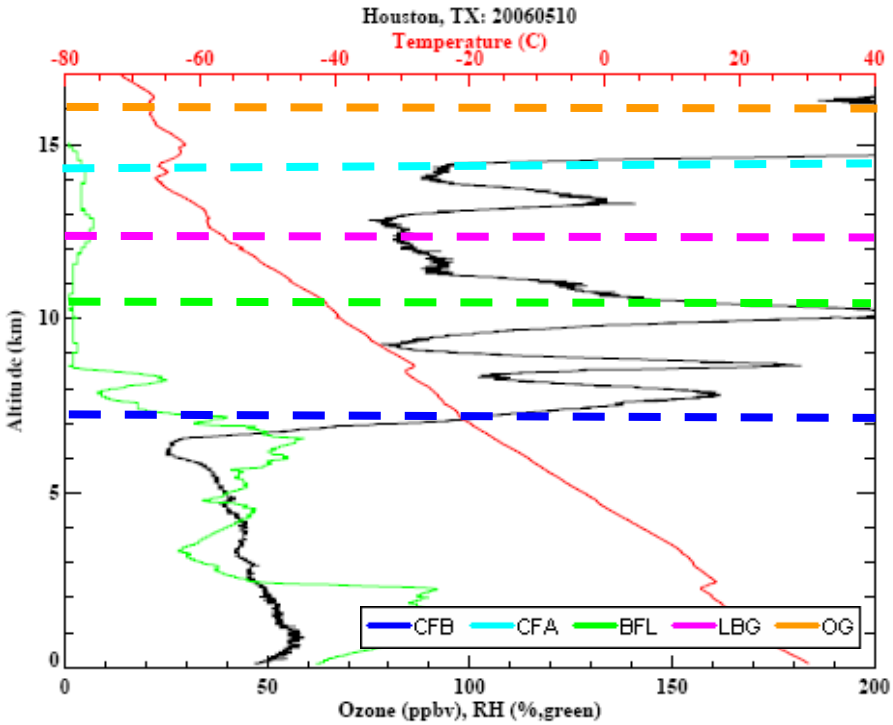

Figure 20. Sounding from Houston, TX on May 10, 2006. The ozonopauses calculated by five different methods are marked with dashed lines as denoted in the legend.

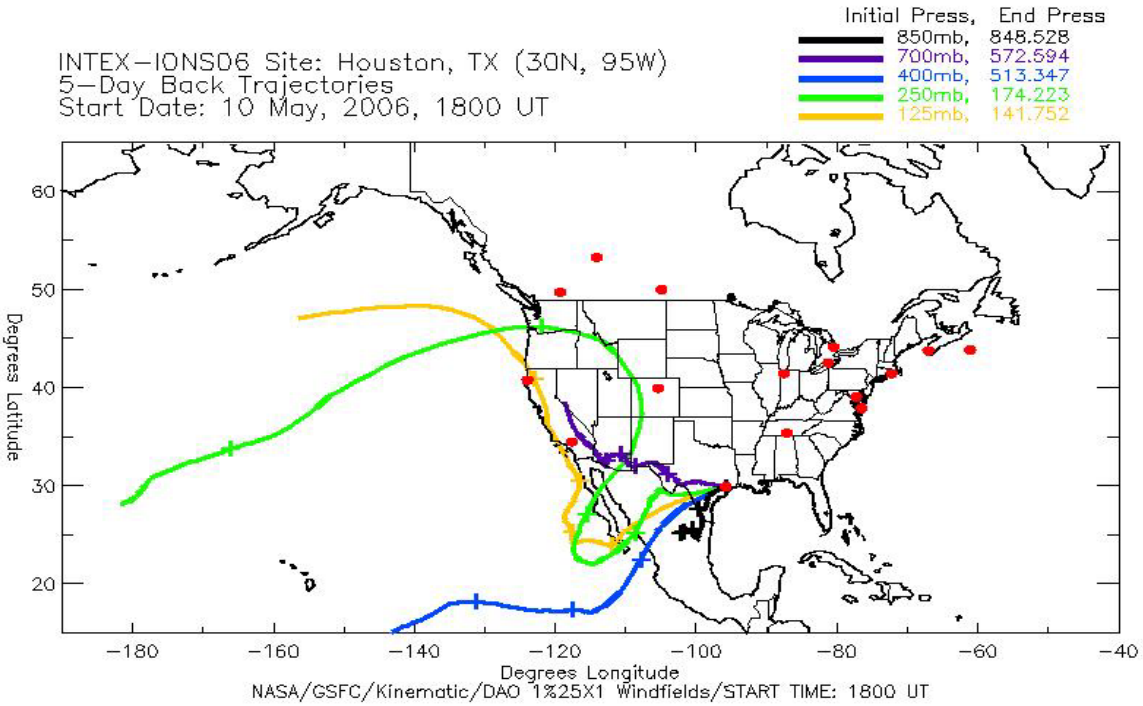

Figure 21. (from croc.gsfc.nasa.gov/intexb) Five-day back trajectories initialized at 18Z on May 10, 2006.

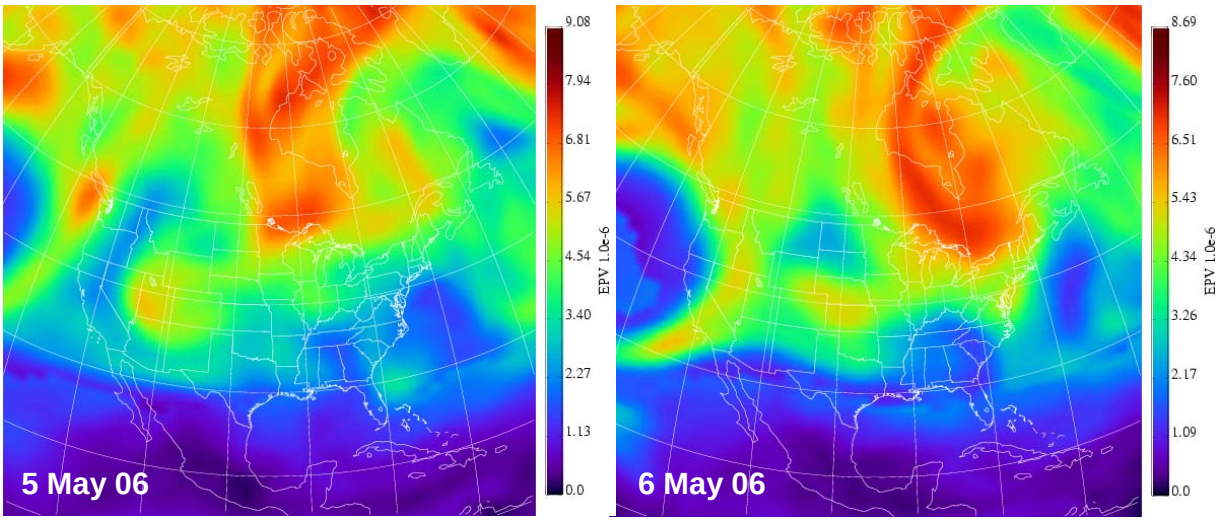

Figure 22. Ertel's potential vorticity (EPV) plots for May 5, 2006 and May 6, 2006.

Strat ozone, weather maps (not included) illustrate the passage of a cold front before the ozonesonde launch. Tropopause fold events often occur on the back side of cold fronts, and these events mix stratospheric air down into the troposphere. The stratospherically injected ozone layers cause the CFB and CFA methods to differ by over 7 km in the placement of the ozonopause. Above the Strat ozone laminae, the ozone concentration drops below 100 ppbv. The CFB, BFL, and LBG methods are deceived by the high ozone concentrations.

Spring and summer ozone profiles often have distinct differences especially near the ozonopause, and so an analysis of the summer ozone profiles is conducted in the same way as in the spring. Figure 23 displays the ozonopause for each of the summer launches over Narragansett, Kelowna, and Houston. The OG method consistently places the ozonopause higher than the other four methods. This method leads to the highest ozonopause in 96% of the 70 total summer ozonesonde launches. The CFB method leads to exceptionally low ozonopauses on multiple summer days in Narragansett, Kelowna, and Houston. As seen in the spring examples, the exceptionally low ozonopauses are caused by high ozone spikes in the middle troposphere. These spikes become more frequent in the summer months because summer is the peak ozone season. In the summer there is ample sunlight to produce hydroxyl radicals that ultimately lead to the formation of ozone. Also, natural VOC emissions are high in the summer because the temperatures are appropriate for tree growth. It is visually obvious that there is more variation in the

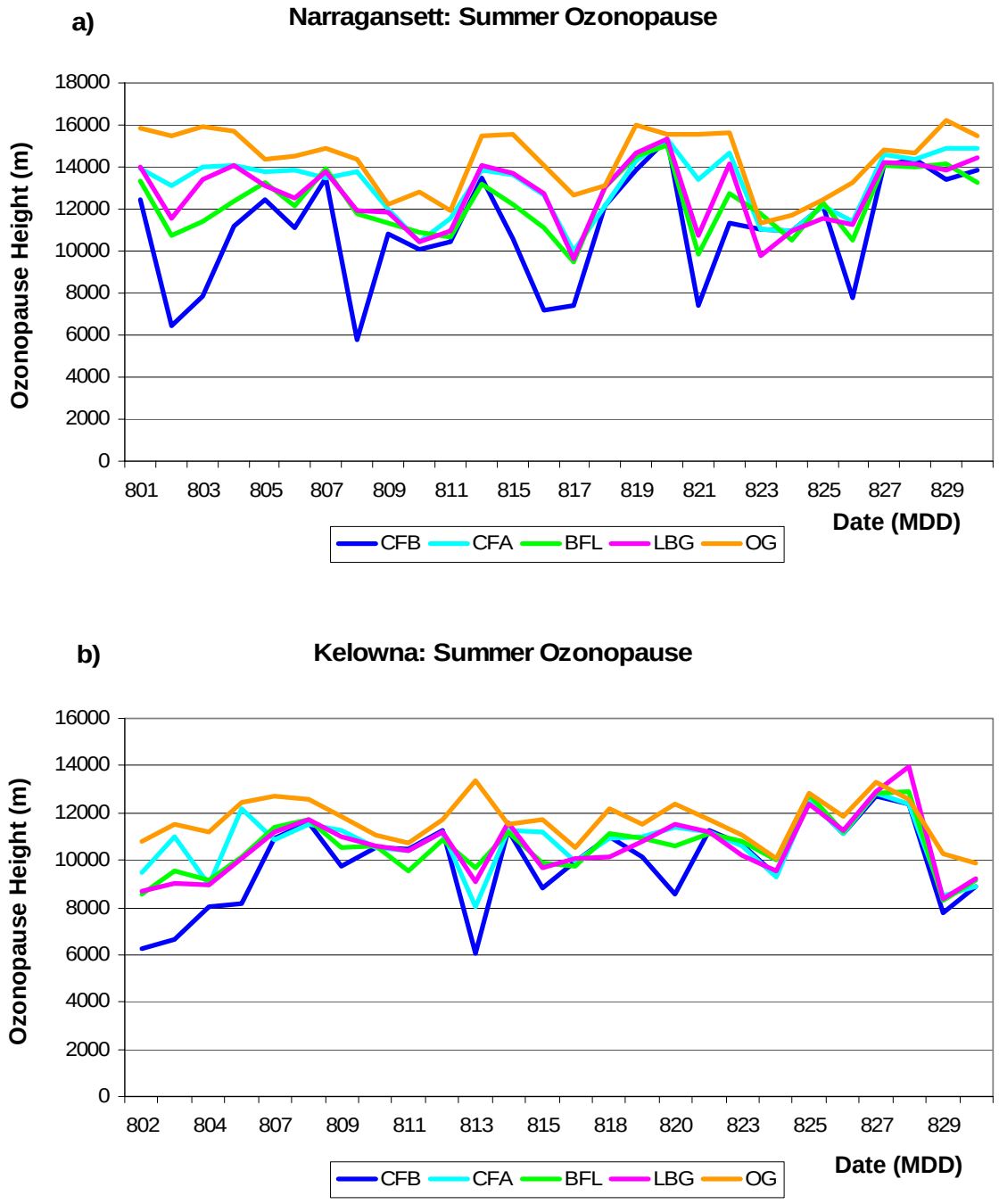

Figure 23 (a, b). Summer ozonopause heights determined by five different methods for Narragansett and Kelowna. CFB = cutoff from below method (dark blue), CFA = cutoff from above method (cyan) , BFL = best fit line method (green), LBG = latitudinally-based groups method (pink), OG = ozone gradient method (orange).

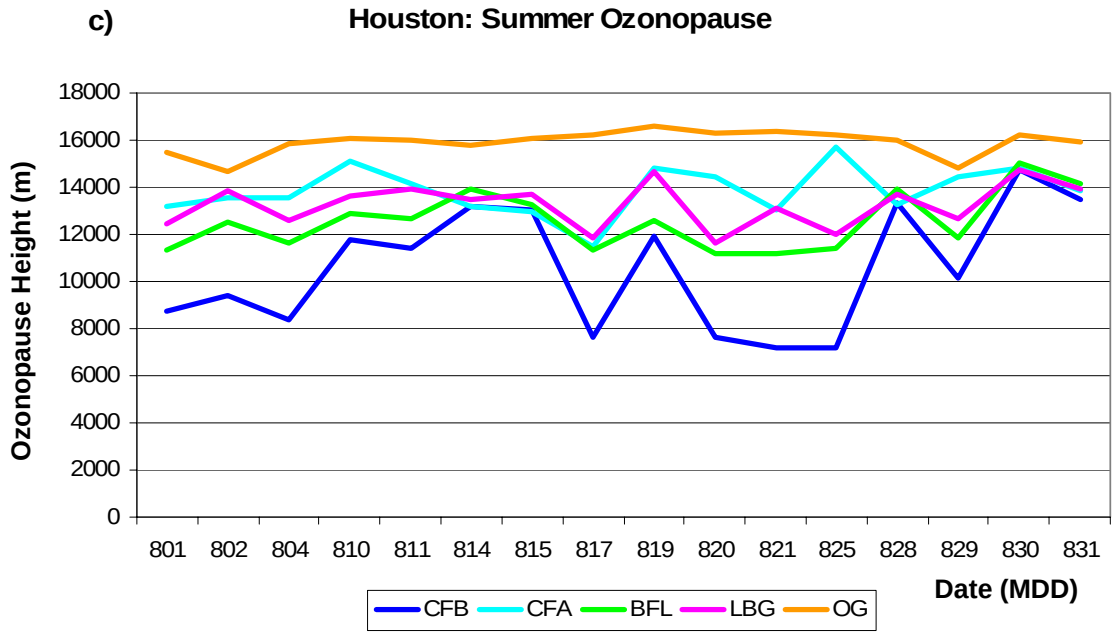

Figure 23 (c). Summer ozonopause heights determined by five different methods for Houston. CFB = cutoff from below method (dark blue), CFA = cutoff from above method (cyan) , BFL = best fit line method (green), LBG = latitudinally-based groups method (pink), OG = ozone gradient method (orange).

ozonopause placements in the summer as compared with the spring. Correlations (Table 4) and histograms of the standard deviations (Fig. 24) confirm this observation. The mean correlations are 0.69 for Narragansett, 0.71 for Kelowna, and 0.34 for Houston. These values are all lower than the correlations found for the spring launches. Kelowna is again the most well-correlated of all of the three sites, and Houston is the least-correlated.

The average standard deviation for Narragansett is 1.5 km (approximately 12% of the average ozonopause height), and the average standard deviation for Kelowna is 0.90 km (approximately 8% of the average ozonopause height). For Houston, the average standard deviation is 2.0 km (approximately 15% of the average ozonopause height).

a) Narragansett summer: correlations between ozonopause methods

	CFB	*CFA*	*BFL*	*LBG*	*OG*
CFB	1.0				
CFA	0.5	1.0			
BFL	0.8	0.7	1.0		
LBG	0.7	0.9	0.9	1.0	
OG	**0.2**	0.9	0.5	0.8	1.0

b) Kelowna summer: correlations between ozonopause methods

	CFB	*CFA*	*BFL*	*LBG*	*OG*
CFB	1.0				
CFA	0.7	1.0			
BFL	0.9	0.8	1.0		
LBG	0.8	0.8	0.9	1.0	
OG	**0.3**	0.6	0.7	0.6	1.0

c) Houston summer: correlations between ozonopause methods

	CFB	*CFA*	*BFL*	*LBG*	*OG*
CFB	1.0				
CFA	**0.1**	1.0			
BFL	1.0	**0.1**	1.0		
LBG	0.8	**0.2**	0.8	1.0	
OG	**0.1**	**0.1**	**0.1**	**0.1**	1.0

Table 4. Correlations between ozonopause heights calculated from each of the five ozonopause methods for summer launches over Narragansett, Kelowna, and Houston. Bold values represent poor correlations ($r < 0.5$).

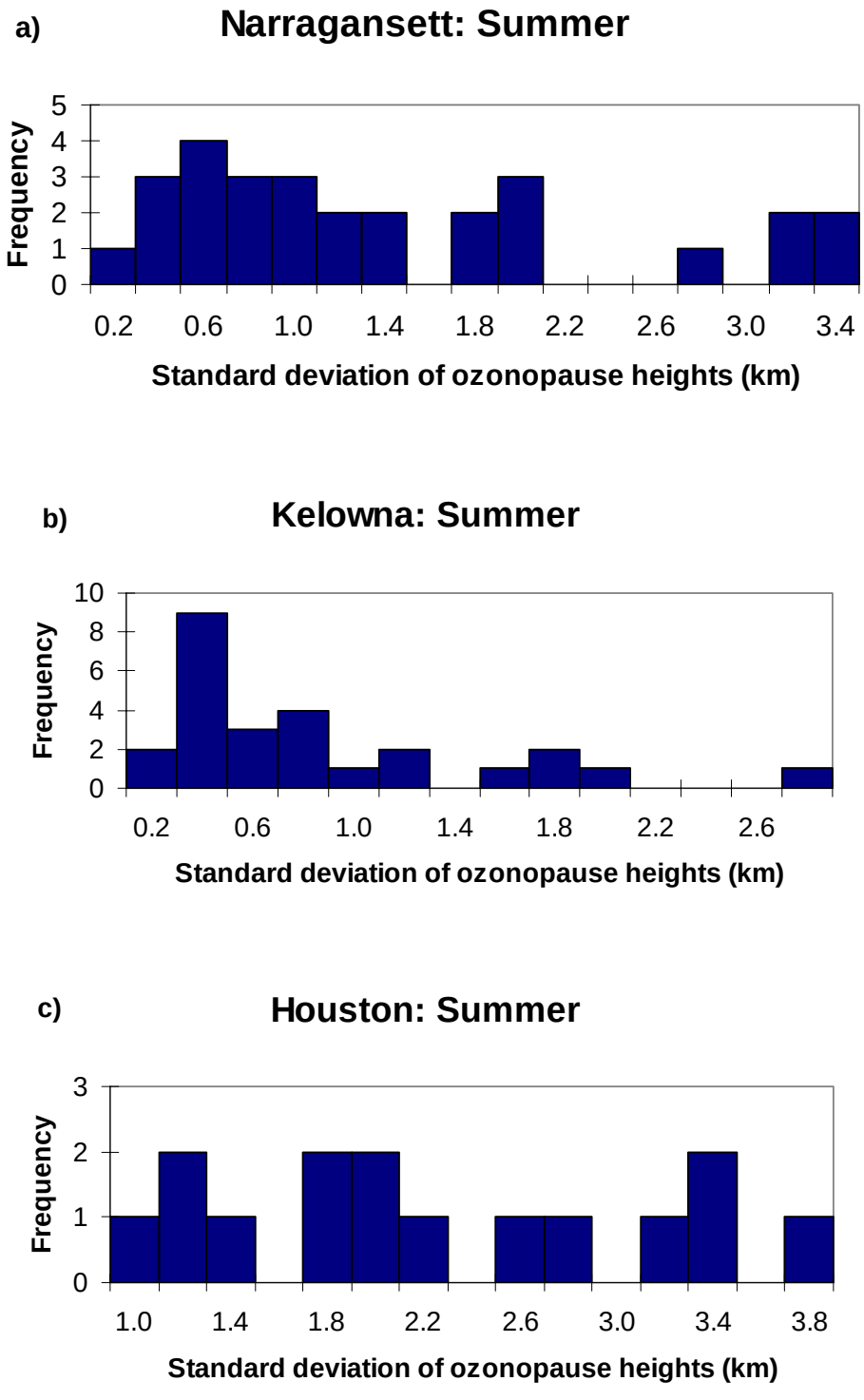

Figure 24. Histograms for Narragansett, Kelowna, and Houston that show the distributions of the standard deviations from the mean of the five ozonopauses in the summer.

The standard deviations as a percentage of the average ozonopauses for Narragansett and Kelowna remained relatively constant between spring and summer. The standard deviations increased significantly in Houston in the summer confirming the observation that the ozonopauses are less similar in the summer.

In Fig. 23b, August 13 (sounding shown in Fig. 25) stands out because the OG method is the only method that does not show a lower ozonopause than the previous day.

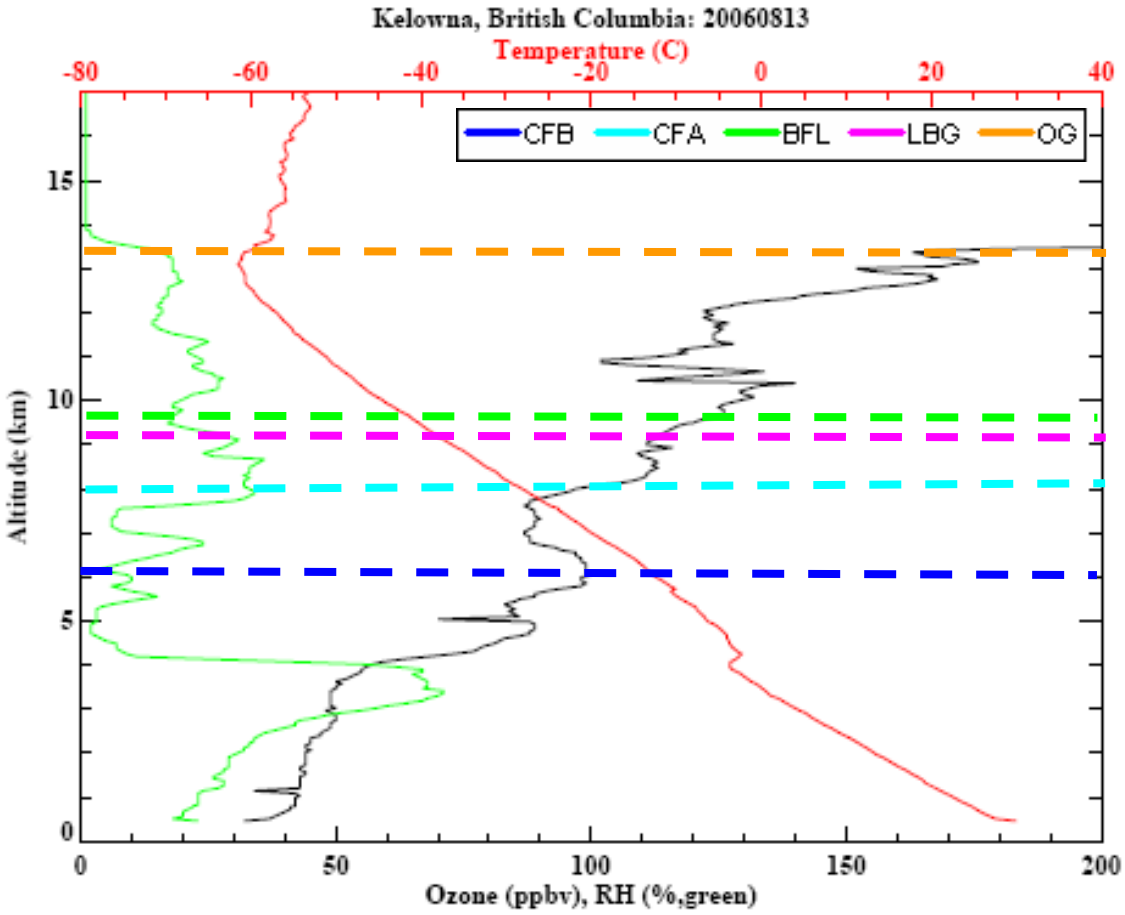

Figure 25. Sounding from Kelowna, BC on August 13, 2006. The ozonopauses calculated by five different methods are marked with dashed lines as denoted in the legend.

Figure 25 is an unusual sounding for Kelowna. In cases in which there is not a sharp ozone gradient, it is difficult to place the ozonopause regardless of the ozonopause calculations used. Based on the five ozonopause heights above and the temperature profile, the OG method best identifies the ozonopause.

The gradual rise in ozone concentrations near the ozonopause seen in Fig. 25 is more representative of the summertime ozone profiles for Houston. Figure 26 is a typical summertime profile over Houston. It explains one of the primary reasons why the five ozonopause methods lead to different ozonopause heights over Houston.

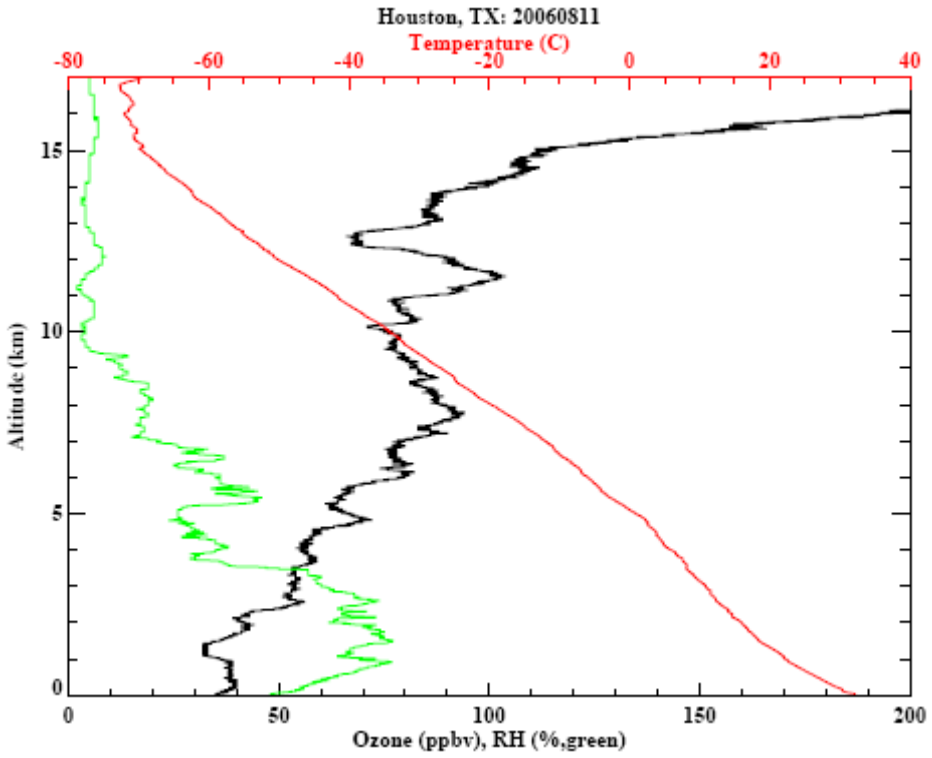

Figure 26. Sounding from Houston, TX on August 11, 2006. Ozone concentrations gradually increase in the upper troposphere, but there is no defined ozonopause.

Dynamically active regions such as the area around Kelowna often see large concentrations of fresh ozone from the stratosphere. This ozone leads to a sharp gradient in the ozone concentrations that allows the ozonopause to be clearly seen. Less dynamically active regions such as the area around Houston often have more aged and mixed ozone near the ozonopause. The ozonopause methods do not agree on one ozonopause height when the ozonopause is not clearly defined.

When the ozonopause placements differ for a particular day, each ozonopause can lead to different TTOCs. Depending on how the categories of ozone are distributed throughout the column, the tropospheric ozone budgets can differ for each ozonopause. In the next section, the tropospheric ozone budgets that result from each ozonopause placement are analyzed.

3.2 Comparisons of Tropospheric Ozone Budgets

The TTOCs for the five ozonopause methods are calculated for each ozonesonde launch. Figure 27 depicts the spring TTOCs over Narragansett. The TTOC is reported in Dobson units (1 DU = 2.69 x 10^{16} cm^{-2}). Figure 27 closely resembles Fig. 15a (the ozonopause heights over Narragansett in the spring). The figure provides evidence for what is intuitively clear: a higher ozonopause leads to a greater TTOC, and a lower ozonopause leads to a smaller TTOC. Figure 28, the summer TTOCs over Houston, provides further evidence. The spring TTOCs for Kelowna and Houston as well as the

summer TTOCs for Narragansett and Kelowna resemble their corresponding ozonopause graphs. The figures are not included in this thesis.

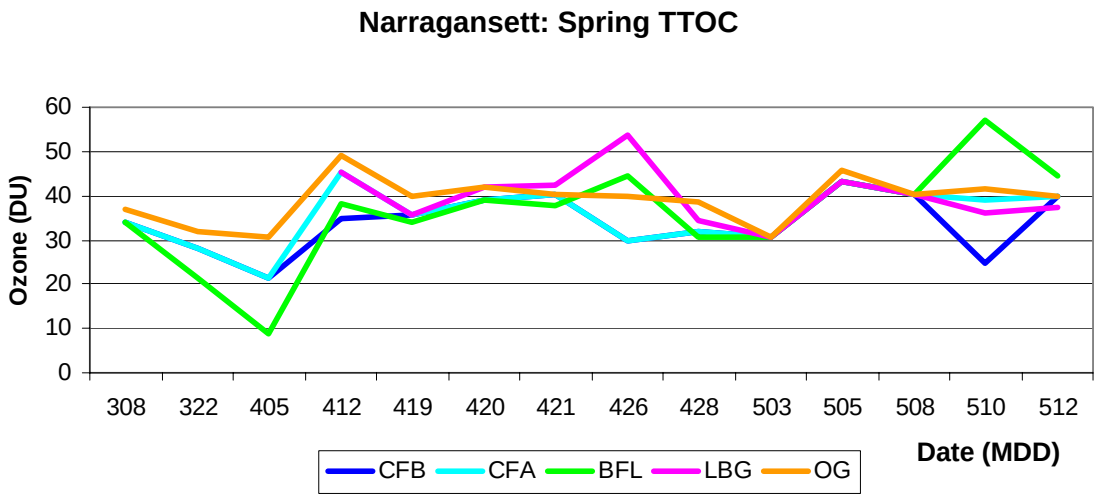

Figure 27. Spring tropospheric ozone columns (in DU) derived from five different ozonopause calculation methods for Narragansett.

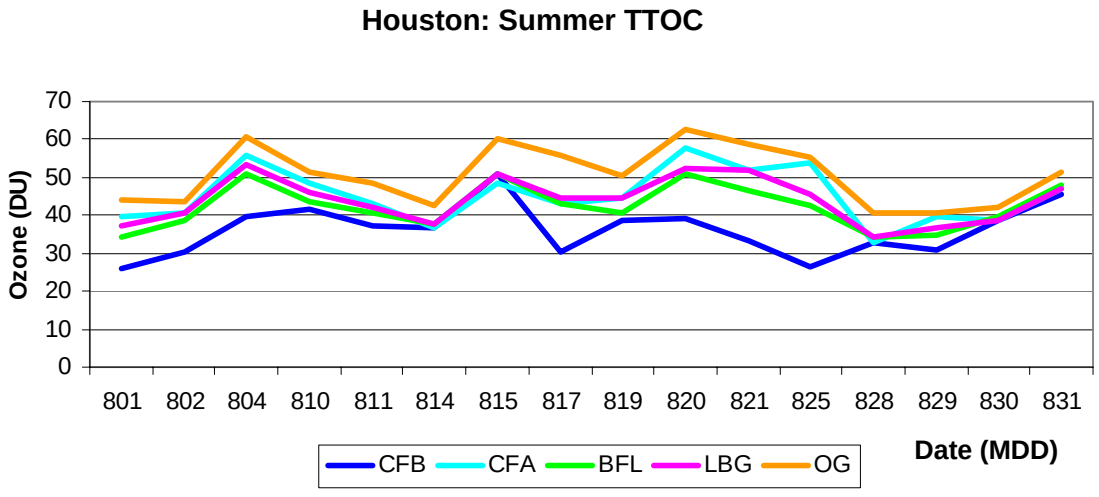

Figure 28. Summer tropospheric ozone columns (in DU) derived from five different ozonopause calculation methods for Houston.

The average spring tropospheric ozone budgets for each site are shown in Fig. 29 as a percentage of the TTOC determined by each ozonopause height. At all three sites in the spring, the variation is less than 5% of the TTOC within each category. The average summer tropospheric ozone budgets for each site are shown in Fig. 30. The variations in the summer are also less than 5% of the TTOC within each category.

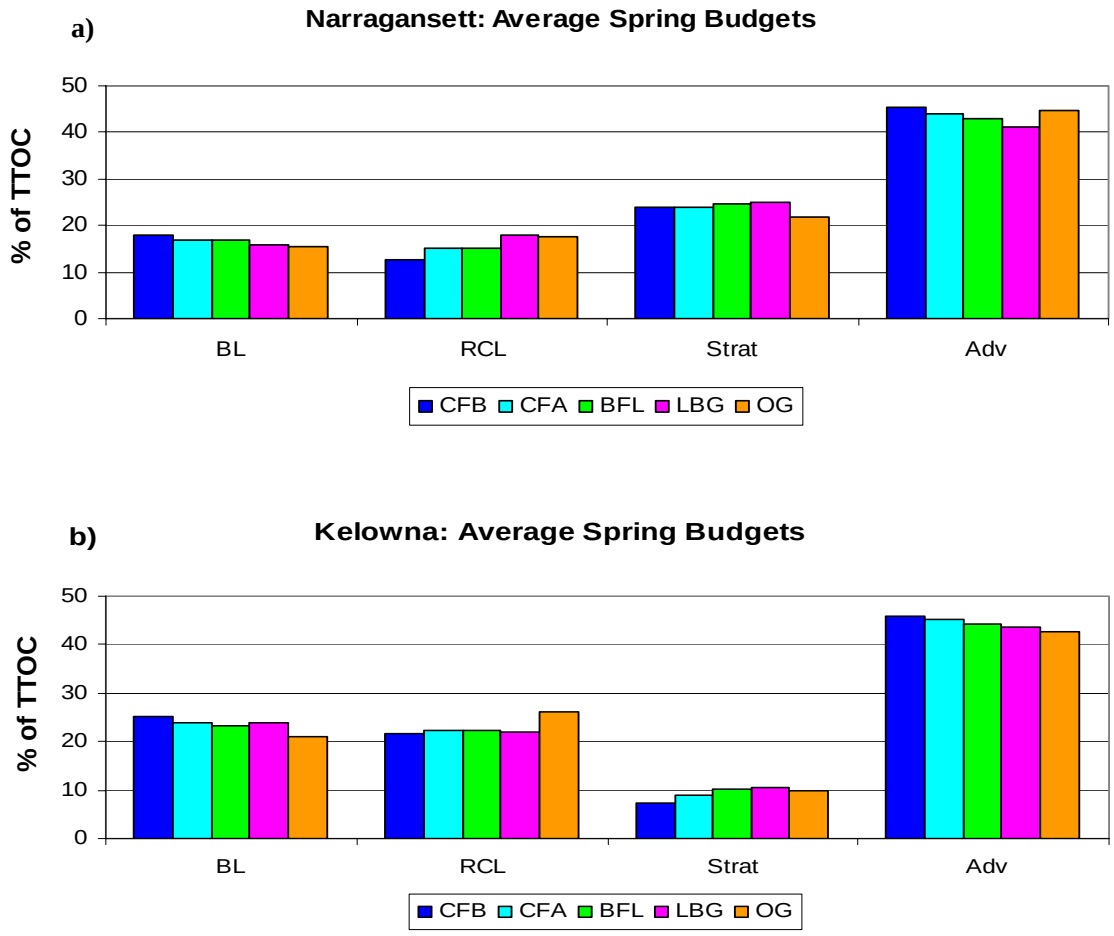

Figure 29 (a, b). Average tropospheric ozone budgets for spring launches over Narragansett and Kelowna. Each category is reported as a percent of the TTOC determined by five ozonopause calculations.

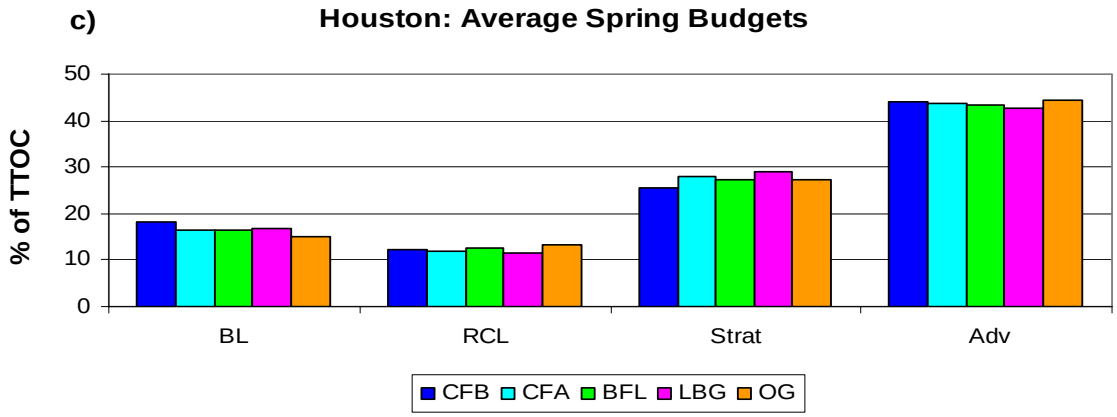

Figure 29 (c). Average tropospheric ozone budgets for spring launches over Houston. Each category is reported as a percent of the TTOC determined by five ozonopause calculations.

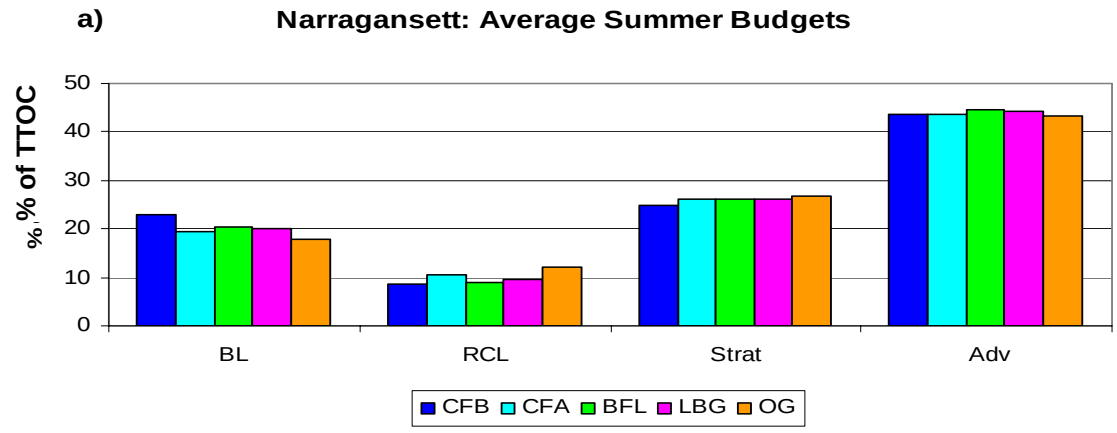

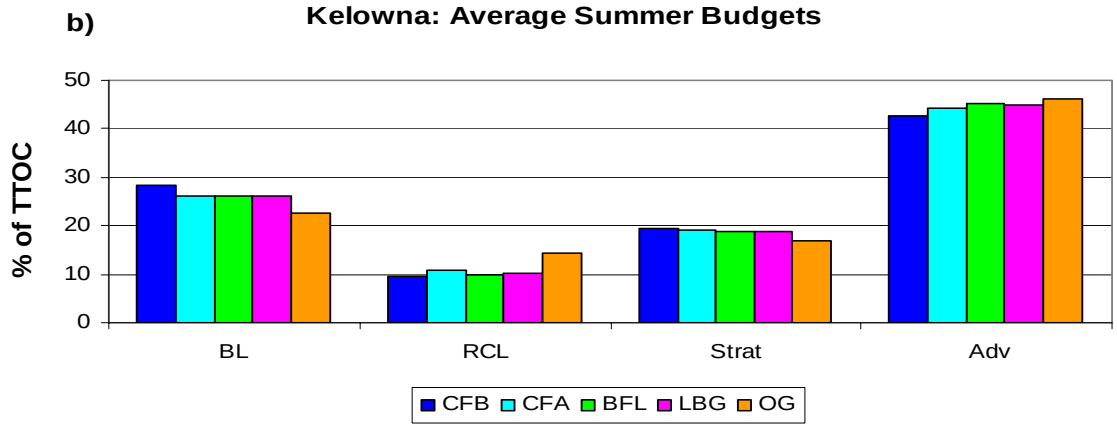

Figure 30 (a, b). Average tropospheric ozone budgets for summer launches over Narragansett and Kelowna. Each category is reported as a percent of the TTOC determined by five ozonopause calculations.

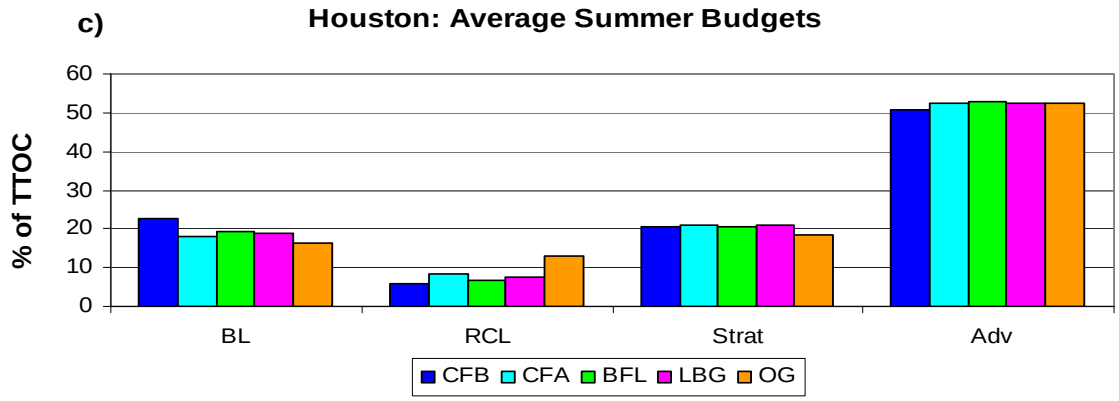

Figure 30 (c). Average tropospheric ozone budgets for summer launches over Houston. Each category is reported as a percent of the TTOC determined by five ozonopause calculations.

In all of the average seasonal budgets except for the Narragansett spring budgets, the OG method yields the highest RCL contribution. In Fig. 31, Loucks (2007) examines the frequency of gravity waves as a function of altitude in the tropics. She concludes that GW-induced laminae are most frequent between 13 and 20 km. If this pattern holds outside of the tropics, then it could be the reason why the RCL contribution is the highest when the ozonopause is the highest. The ozonopauses for Narragansett, Kelowna, and Houston do not reach 20 km on any day, but the ozonopauses frequently reach 13 km, especially in Houston. Further investigations will have to be conducted to determine if a similar GW frequency pattern is present in the selected IONS-06 sites.

Figures 29 and 30 show that either the outlier methods from the ozonopause graphs (Figures 15 and 23) are not affecting the mean owing to the large sample size or that the ozonopause placement does not have a large impact on the tropospheric ozone budgets. In order to test these two theories, specific days must be examined. In Section

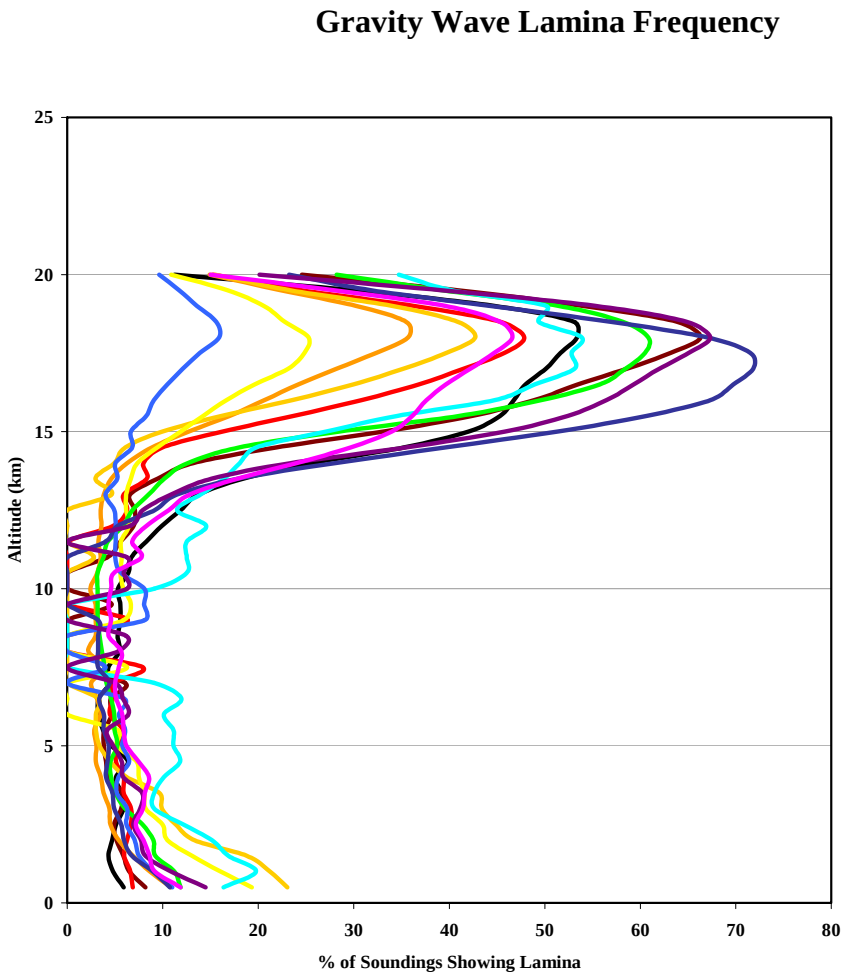

Figure 31. (From Loucks 2007) Frequency of GW-induced laminae as a function of altitude for 12 tropical sites.

3.1, May 10 over Narragansett is identified as a day having large variations in the ozonopause placement given by the five methods. The ozonopause height ranges from 5.6 km (CFB method) to 12.1 km (BFL method), but the other three methods lead to ozonopauses clustered around 10 km (see Fig. 17). The May 10 ozone budgets for each of the five methods are displayed in Fig. 32. The CFB method did not find any RCL ozone.

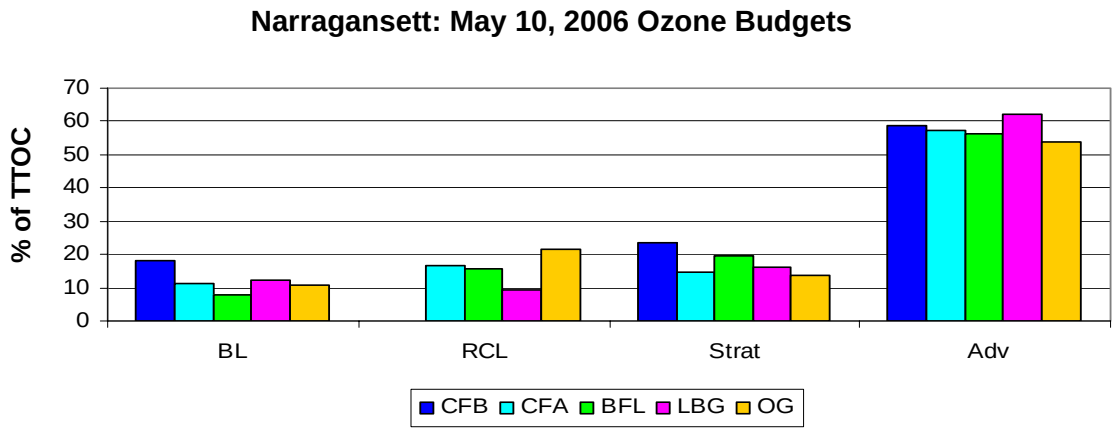

Figure 32. Tropospheric ozone budgets for the May 10, 2006 ozonesonde launch over Narragansett.

Differences are more apparent in the daily ozone budget than in the seasonal ozone budget. Comparing the actual amounts of ozone in each of the ozone budget categories is also useful. Table 5 indicates that four of the ozonopause methods lead to 5.8 DU of Strat ozone. The percentages vary from 13% to 23% because the amount of ozone in the TTOC varies from 24.7 DU to 41.6 DU among these methods. As discussed above, the CFB and BFL ozonopauses do not provide accurate representations of the transition between the stratosphere and the troposphere. Even if these two methods are ignored, the RCL term still ranges between 9% and 21% when the three tropopauses differ by less than 1 km. Table 5 indicates that there are thin GW-induced layers that lie between the ozonopauses determined by the CFA, LBG, and OG methods.

Table 5. Ozone (in DU) in each category for the five ozonopauses over Narragansett on May 10, 2006.

	BL	RCL	Strat	Adv	TTOC
CFB	4.5	0.0	5.8	14.5	24.7
CFA	4.5	6.5	5.8	22.4	39.1
BFL	4.5	9.0	11.3	32.1	56.9
LBG	4.5	3.4	5.8	22.4	36.0
OG	4.5	9.0	5.8	22.4	41.6

Figure 18 in Section 3.1 is a sounding from Kelowna on April 26. Four of the methods lead to ozonopauses that are less than 1 km apart from the highest to the lowest. The CFB method incorrectly identifies a spike in ozone concentrations as the ozonopause. The ozone budgets for the other four methods show little or no variations (<1 %) within each group. Because the ozone budgets did not change, ozonopause placement is not significant in the tropopause region in this case. This is an important finding because the ozonopause in this profile is difficult to quantify owing to the lack of a sharp gradient in ozone concentrations.

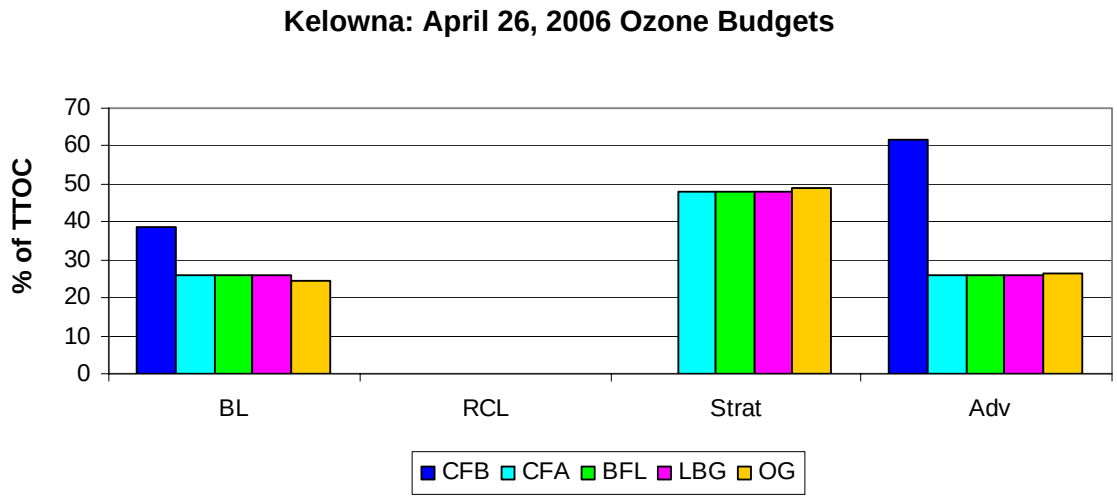

Figure 33. Tropospheric ozone budgets for the April 26, 2006 ozonesonde launch over Kelowna.

Profiles over Houston routinely exhibit a gradual increase in ozone concentrations near the in the upper troposphere as in the previous Kelowna example. One of these cases is the March 13, 2006 Houston profile (Fig. 34) that is examined to determine if the ozone budgets are affected by the tropopause placement. The ozone budgets for this day are depicted in Fig. 35.

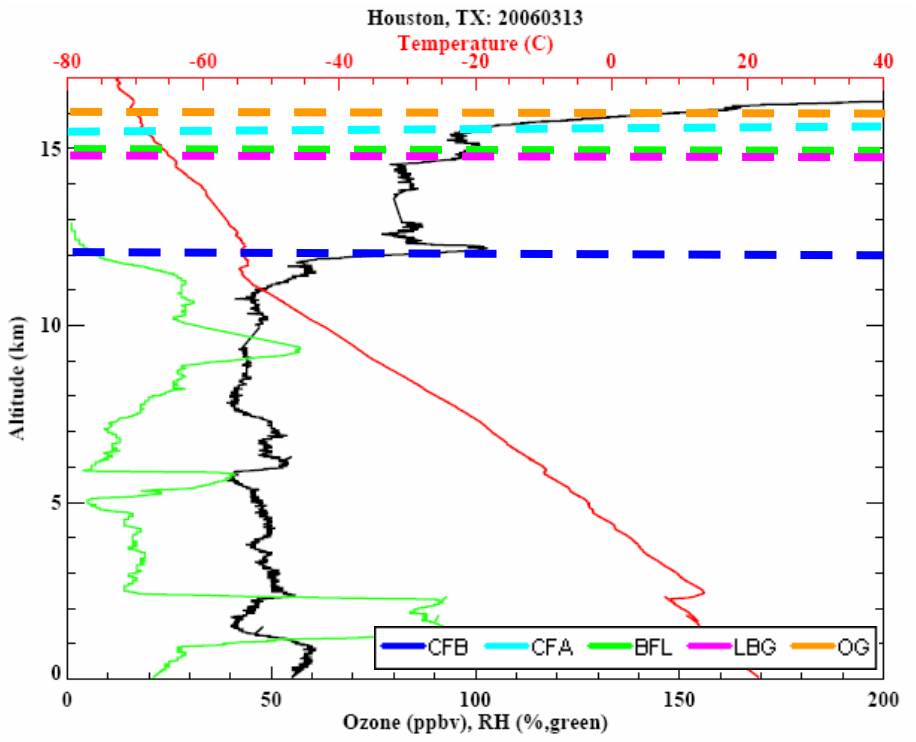

Figure 34. Sounding from Houston, TX on March 13, 2006. The ozonopauses calculated by five different methods are marked with dashed lines as denoted in the legend.

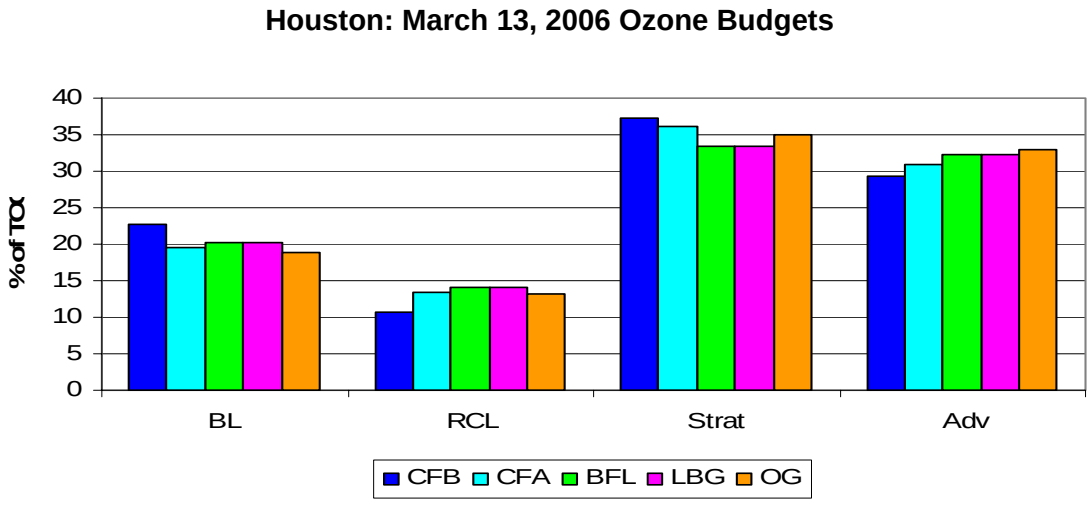

Figure 35. Tropospheric ozone budgets for the March 13, 2006 ozonesonde launch over Houston.

The standard deviation from the mean of the five ozonopauses is 1.6 km. Again the CFB ozonopause is lower than the other four. If the CFB ozonopause is ignored, then the standard deviation is 0.6 km. The variations in the ozone budgets are larger than the variations in the previous Kelowna example. Even still, the percentages within each category vary by less than 3% of the TTOC. This example illustrates that the ozonopause placement does affect ozone budgets in some cases. Further case studies are necessary to understand the reasons why the normalized budgets are not sensitive to ozonopause placements in some cases.

Chapter 4. SUMMARY AND CONCLUSIONS

This study uses data from ozonesonde launches over Narragansett, Rhode Island; Kelowna, British Columbia; and Houston, Texas to investigate five different ozonopause calculation methods. These three sites are chosen in order to test the methods on a variety of climates, elevations, and latitudes. The ozonesonde launches occurred in the mid-afternoon during the IONS field campaigns in the spring and summer of 2006. Two of the five ozonopause methods are developed for this study, and three of the methods are from other publications. The five methods use an ozone concentration cutoff, a best fit line, or an ozone gradient to place the ozonopause. Variations in the ozonopause placements are dependent on the site and the season. The ozonopauses match the best for the spring profiles over Kelowna where the average standard deviation from the mean of the five profiles is 0.82 km (approximately 8% of the average ozonopause). The ozonopauses differ the most for the summer profiles over Houston where the average standard deviation from the mean of the five profiles is 2.0 km (approximately 15% of the average ozonopause). Discrepancies in the ozonopause placements are seen primarily when there are large spikes of ozone in the middle troposphere or when there is not a distinct ozonopause. Out of all three sites, these issues arise most frequently in Houston; out of the two seasons, these issues arise more frequently in summer.

There is rarely only one correct ozonopause placement, and so profiles from individual days are examined to determine which methods clearly do *not* work. The

method that is least accurate based on visual assessments of the profiles is the method that searches from the middle of the profile to find a predetermined ozone concentration cutoff. The methods that are most accurate are the method based on gradients of ozone and the method that searches from the top of the profile down to a predetermined ozone concentration cutoff.

The five ozonopause methods are used to calculate five tropospheric ozone columns (TTOCs) for each of the ozonesonde launches. Then, using a laminar identification method, the TTOCs are divided into four categories: boundary layer ozone, regional convection and lightning generated ozone, stratospherically-injected ozone, and recently advected or aged ozone. The combination of these categories is called a tropospheric ozone budget. These budgets are compared to determine the effect of ozonopause placement on tropospheric ozone budgets. Seasonal averages for each site show little variation in the relative contributions of each term (<5 % of the TTOC). Daily comparisons of the ozone budgets show larger variations, especially when the ozonopause calculation methods lead to significantly different ozonopauses. Daily comparisons also show that the placement of the ozonopause when there is not a sharp gradient in ozone concentrations may not be significant, as long as the ozonopause intersects the gradual rise of the concentrations.

Future work will expand the tropopause investigation to include more of the IONS-06 sites, such as Mexico City and Boulder. Both of these sites are elevated and are

located in regions not covered in this thesis. With a larger data set, the ozone gradient method developed for this thesis can be fine-tuned to work for all of the IONS-06 sites.

This thesis uses boundary layer heights estimated from mean ozonesonde profiles and boundary layer heights of meteorologically and geographically similar sites. Future work includes determining an accurate method for calculating the boundary layer depth, especially over Kelowna. The estimated boundary layer depth for Kelowna is 2.4 km in the spring and 2.9 km in the summer. This boundary layer is fairly deep, and if it is inaccurate, then the tropospheric ozone budgets may not represent the categories of ozone accurately.

Other future work includes calculating the frequency of gravity waves and Rossby waves as a function of height for each site, as in Loucks (2007). These values would help to explain the variability of the tropospheric ozone budgets in Section 3.2.

REFERENCES

Angevine, W. M., J. E. Hare, C. W. Fairall, et al. (2006), Structure and formation of the highly stable marine boundary layer over the Gulf of Maine, *J. Geophys. Res.*, *111*, D23S22, doi:10.1029/2006JD007465.

Baird, C. and M. Cann (2005). Environmental Chemistry, W. H. Freeman and Company, New York.

Bell, M. L., A. McDermott, S. L. Zeger, *et al*. (2004), Ozone and short-term mortality in 95 US urban communities, 1987-2000, *J. Am. Med. Assoc.*, *292*, 2372-2378.

Birner, T. (2006), Fine-scale structure of the extratropical tropopause region, *J. Geophys. Res.*, *111*, D04104, doi: 10.1029/2005JD006301.

Choi, Y., Y. H. Wang, T. Zeng, *et al.* 2005, Evidence of lightning NO_x and convective transport of pollutants in satellite observations over North America, *Geophys. Res. Lett.*, *32*, L02805, doi:10.1029/2004GL021436.

Cooper, O.R., A. Stohl, M. Trainer, *et al.* (2006), Large upper tropospheric ozone enhancements above mid-latitude North America during summer: In situ evidence from the IONS and MOZAIC ozone measurement network, *J. Geophys. Res.*, *111*, D24S05, doi:10.1029/2006JD007306.

Diab, R. D., A. Raghunandan, A. M. Thompson, and V. Thouret (2003), Classification of tropospheric ozone profiles over Johannesburg based on mosaic aircraft data, *Atmos. Chem. Phys.*, *3*, 713-723.

Dobson, G. M. B. (1973), The laminated structure of the ozone in the atmosphere, *Q. J. R. Meteorol. Soc.*, *99*, 599-607.

Fiore, A. M., D. J. Jacob, I. Bey, *et al.* (2002), Background ozone over the United States in summer: origin, trend, and contribution to pollution episodes, *J. Geophys. Res.*, *107* (D15), 4275, doi:10.1029/2001JD000982.

Grant, W. B., R. B. Pierce, S. J. Oltmans, and E. V. Browell (1998), Seasonal evolution of total and gravity wave induced laminae in ozonesonde data in the tropics and subtropics, *Geophys. Res. Lett.*, *43*, 1863-1866.

Hoerling, M. P., T. K. Schaack, and A. J. Lenzen (1991), Global objective tropopause analysis, *Mon. Weather Rev*., *119*, 1816– 1831.

Holton, J. R. (1987), The production of temporal variability in trace constituents concentrations, in *Transport processes in the middle atmosphere*, D. Reidel Publishing Company, 313-326.

Holzworth, G. C. (1972), Mixing heights, wind speeds, and potential for urban air pollution throughout the contiguous United States, Environmental Protection Agency, Research Triangle Park, North Carolina.

Hsu, J. and M. J. Prather (2005), Diagnosing the stratosphere-to-troposphere flux in a chemistry transport model, *J. Geophys. Res., 110*, D19305, doi:10.1029/2005JD006045.

Hudman, R. C., D. J. Jacob, S. Turquety, *et al.* (2007), Surface and lightning sources of nitrogen oxides in the United States: Magnitudes, chemical evolution, and outflow, *J. Geophys. Res., 112*, D12S05, doi:10.1029/2006JD007912.

Kaynak, B., Y. Hu, R. V. Martin, *et al.* (2008), The effect of lightning NO_x production on surface ozone in the continental United States, *Atmos. Chem. Phys. Discuss., 8*, 5061-5089.

Kasibhatla, P., W. L. Chameides, R. D. Saylor, and D. Olerud (1998), Relationships between regional ozone pollution and emissions of nitrogen oxides in the eastern United States, *J. Geophys. Res., 103*, 22 663–22 669.

Law, K., L. Pan, H. Wernli, *et al.*, (2005), Processes governing the chemical distribution of the extra-tropical UTLS, *IGAC Newsletter*, no. 32.

Loucks, A. (2007), Evaluation of dynamical sources of ozone laminae in tropical troposphere and tropical tropopause layer, State College, The Pennsylvania State University, Department of Meteorology, Master's thesis.

Merrill, J. T., J. L. Moody, S. J. Oltmans, and H. Levy III (1996), Meteorological analysis of tropospheric ozone profiles at Bermuda, *J. Geophys. Res., 29*, 201-212.

Morris, G. A., S. Hersey, A. M. Thompson, *et al*. (2006), Alaskan and Canadian forest fires exacerbate ozone pollution over Houston, Texas, on 19 and 20 July 2004, *J. Geophys. Res., 111*, D24S03, doi: 10.1029/2006JD007090.

Pan, L. L., K. P. Bowman, M. Shapiro, *et al.* (2007), Chemical behavior of the tropopause observed during the Stratosphere-Troposphere Analyses of Regional Transport experiment, *J. Geophys. Res., 112*, D18110, doi:10.1029/2007JD008645.

Pierce, R. B. and W. B. Grant (1998), Seasonal evolution of Rossby and gravity wave induced laminae in ozonesonde data obtained from Wallops Island, Virginia, *Geophys. Res. Lett., 43*, 1859-1862.

Postel, G. A. and Hitchman, M. H. (1999), A climatology of Rossby wave breaking along the subtropical tropopause, *J. Atmos. Sci., 56*, 359-373.

Randel, W. J., D. J. Seidel, and L. L. Pan (2007), Observational characteristics of double tropopauses, *J. Geophys. Res., 112*, D07309, doi:10.1029/2006JD007904.

Reid, S. J. and G. Vaughn (1991). Lamination in ozone profiles in the lower stratosphere, *Q. J. R. Meteorol. Soc., 117*, 825-844.

Stajner, I., K. Wargan, S. Pawson, *et al.* (2007), Assimilated ozone from EOS-Aura: evaluation of the tropopause region and tropospheric columns, in press.

Statistics Canada (2006), Census 2006 (available at http://www12.statcan.ca/english/census/index.cfm, accessed 3/5/08).

Stone, J. (2006), Regional variability of Rossby wave-influenced ozone in the troposphere, State College, The Pennsylvania State University, Department of Meteorology, Master's thesis.

Stull, Roland B. (1988), *An Introduction to Boundary Layer Meteorology*, Kluwer Academic Publishers, Dordrecht, The Netherlands.

Teitelbaum, H. (1996), The role of atmospheric waves in the laminated structure of ozone profiles at high latitude. *Tellus, 49*, 442-455.

Texas Commission on Environmental Air Quality (TCEQ), Houston-Galveston-Brazoria Eight-Hour Ozone Nonattainment Area (available at www.tceq.state.tx.us, accessed on 3/5/08).

Thompson, A. M., J. Stone, J. C. Witte, *et al.* (2007a), IONS (INTEX Ozonesonde Network Study, 2004): 1. Summertime upper troposphere/lower stratosphere (UT/LS) ozone over northeastern North America, *J. Geophys. Res., 112*, D12S13: doi: 10.1029/2006JD007441.

Thompson, A. M., J. Stone, J. C. Witte, *et al.* (2007b), IONS (INTEX Ozonesonde Network Study, 2004): 1. Tropospheric ozone budgets and variability over northeastern North America, *J. Geophys. Res., 112*, D12S13: doi: 10.1029/2006JD007670.

Thompson, A. M., J. E. Yorks, S. K. Miller, *et al.* (2008), Tropospheric ozone sources and wave activity over Mexico City and Houston during Milagro/Intercontinental Transport Experiment (INTEX-B) Ozonesonde Network Study, 2006 (IONS-06), *Atmos. Chem. Phys., 8,* 1-29.

United States Census Bureau (2000), Population estimates (available at www.census.gov/popest/estimates.php, accessed 3/5/08).

The Weather Channel (TWC), Monthly average temperatures (available at www.weather.com/weather/wxclimatology; accessed 3/5/08).

World Meteorological Organization (1957), Meteorology - a three-dimensional science: second session of the Commission for Aerology, *WMO Bulletin, vol. IV*, no. 4, 134-138.

Yorks, J. E. (2007), The variability of free-tropospheric and boundary layer ozone over Beltsville, MD, State College, The Pennsylvania State University, Department of Meteorology, Master's thesis.

Zhang, R. Y., X. X. Tie, and D. W. Bond (2003), Impacts of anthropogenic and natural NO_x sources over the US on tropospheric chemistry, *P. Natl. Acad. Sci. USA,* 100, 1505–1509.